

NACA TN 3349 7396

TECH LIBRARY KAFB, NM  
0066095

# NATIONAL ADVISORY COMMITTEE FOR AERONAUTICS

TECHNICAL NOTE 3349

APPLICATION OF THE GENERALIZED SHOCK-EXPANSION METHOD  
TO INCLINED BODIES OF REVOLUTION TRAVELING  
AT HIGH SUPERSONIC AIRSPEEDS

By Raymond C. Savin

Ames Aeronautical Laboratory  
Moffett Field, Calif.



Washington  
April 1955

AFM C  
TECHNICAL LIBRARY  
AFL 2811



## NATIONAL ADVISORY COMMITTEE FOR AERONAUTICS

## TECHNICAL NOTE 3349

## APPLICATION OF THE GENERALIZED SHOCK-EXPANSION METHOD

## TO INCLINED BODIES OF REVOLUTION TRAVELING

## AT HIGH SUPERSONIC AIRSPEEDS

By Raymond C. Savin

## SUMMARY

The flow about a body of revolution at high supersonic airspeeds is investigated analytically with the aid of the generalized shock-expansion method. With the assumption that flow at the vertex is conical, approximate solutions for the flow field are obtained for values of the hypersonic similarity parameter (i.e., the ratio of the free-stream Mach number to the fineness ratio of the body) greater than about 1 and for angles of attack less than the semivertex angle of the body. Surface streamlines are approximated by meridian lines and the flow field is calculated in meridian planes. Simple explicit expressions are obtained for the surface Mach numbers and pressures in the special case of slender bodies.

In the case of lifting cones, algebraic solutions defining the entire flow field are obtained when the hypersonic similarity parameter has a value of about 1.4 or greater.

Surface pressures and shock-wave shapes were obtained experimentally at Mach numbers from 3.00 to 5.05 and angles of attack up to  $15^\circ$  for two ogives having fineness ratios of 3 and 5 and for two cones having the same vertex angles as the ogives. The predictions of the methods of this paper are found to be in good agreement with experiment at values of the hypersonic similarity parameter in the neighborhood of 1 and greater, when the ratio of angle of attack to semivertex angle is about one-half, or less. For increasing values of this ratio, agreement deteriorates but may still be considered fair for values slightly less than 1.

## INTRODUCTION

It was suggested in reference 1 that flow over the surface of a non-lifting body of revolution could be treated as two-dimensional in type downstream of the vertex when the hypersonic similarity parameter (i.e., the ratio of the free-stream Mach number to the fineness ratio of the body) was greater than about 1. This point was substantiated by comparing predictions of two-dimensional (Prandtl-Meyer) expansion theory with those of

characteristics theory for the Mach numbers and pressures on the surfaces of ogives. The two-dimensional theory has the advantage, of course, of being relatively simple by comparison to characteristics theory and is about as simple as the recently proposed hypersonic small disturbance theory of Van Dyke (ref. 2).

It was also suggested in reference 1 that the two-dimensional approach might be extended to the calculation of flow at the surface of slightly inclined bodies of revolution. This thought led to a study (ref. 3) of three-dimensional hypersonic flows which revealed that such flows may often appear locally two-dimensional. It was concluded that at hypersonic speeds the entire flow field about a three-dimensional body may, under certain conditions, be calculated with a shock-expansion method similar to that employed for calculating two-dimensional flow about airfoils (ref. 4). The conditions of when and how this generalized shock-expansion method can be applied to calculate three-dimensional flows were determined in reference 3.

The principal objective of the present paper is to apply the generalized shock-expansion method to obtain expressions yielding the Mach number and pressure distributions throughout the entire flow field about an inclined body of revolution. In order to apply the shock-expansion method, it is necessary to know initial conditions at the vertex of a lifting body. These conditions can be taken to be the same as those about a cone tangent to the body at the vertex. One objective of this paper, then, is to develop a conical flow theory for lifting cones over the range of free-stream Mach numbers and apex angles not treated in the M.I.T. tables (ref. 5).

#### NOTATION

|       |  |
|-------|--|
| $a$   | local speed of sound, ft/sec   |
| $C_N$ | normal-force coefficient, $\frac{\text{normal force}}{q_0 \pi (d^2/4)}$                          |
| $c_p$ | specific heat at constant pressure, ft-lb/slug $^{\circ}\text{R}$                                |
| $c_v$ | specific heat at constant volume, ft-lb/slug $^{\circ}\text{R}$                                  |
| $d$   | maximum diameter of body of revolution, in.  |
| $E$   | entropy, ft-lb/slug $^{\circ}\text{R}$   |
| $H$   | total pressure, lb/sq in.  |
| $K$   | hypersonic similarity parameter, $M_0 \frac{d}{l}$   |
| $l$   | characteristic body length (measured from vertex to most forward point of maximum diameter), in. |

|            |   |
|------------|---|
| M          | Mach number (ratio of local velocity to local speed of sound)   |
| p          | static pressure, lb/sq in.  |
| q          | dynamic pressure, lb/sq in.   |
| P          | pressure coefficient, $\frac{p - p_0}{q_0}$   |
| R          | gas constant, ft-lb/slug $^{\circ}$ R   |
| u          | velocity component parallel to ray passing through vertex of cone, ft/sec   |
| v          | velocity component normal to u in a meridian plane, ft/sec  |
| w          | velocity component normal to a meridian plane, ft/sec   |
| V          | resultant velocity, $\sqrt{u^2 + v^2 + w^2}$ , ft/sec   |
| $\hat{V}$  | maximum velocity obtainable by expanding to zero temperature, ft/sec  |
| x          | distance along axis of body measured from vertex, in.   |
| r          | distance normal to axis of body, in.  |
| $\alpha$   | angle of attack, radians unless otherwise specified   |
| $\beta$    | Mach angle, $\arcsin \frac{1}{M}$ , radians unless otherwise specified  |
| $\gamma$   | ratio of specific heats, $\frac{c_p}{c_v}$  |
| $\delta$   | angle of flow inclination in meridian plane measured with respect to body axis, radians unless otherwise specified      |
| $\epsilon$ | angle of inclination of axis of conical shock with respect to free-stream direction, radians unless otherwise specified |
| $\eta$     | angle of inclination of axis of conical shock with respect to axis of body, radians unless otherwise specified          |
| $\rho$     | mass density, slugs/cu ft   |
| $\phi$     | angle of meridian plane with respect to plane of symmetry, radians unless otherwise specified (see fig. 1)              |
| $\omega$   | angle between axis of cone and ray passing through vertex of cone, radians unless otherwise specified                   |

## Subscripts

- o free-stream conditions
- $\left. \begin{matrix} A, B, \\ C, D, \dots \end{matrix} \right\}$  conditions at different points in the flow field
- c conditions on the surface of a cone
- e conditions at the external surface of the vortical layer
- N conditions on the surface at the vertex of a body
- s conditions immediately behind the shock wave at the vertex of a body

## THEORY

This investigation is concerned with the theoretical and experimental characteristics of the flow about bodies of revolution traveling at high supersonic airspeeds and at small angles of attack. It is assumed throughout the analysis that the disturbed flow is everywhere supersonic and, hence, the body has a pointed nose or vertex. With these restrictions on the free-stream Mach number, angle of attack, and body shape, the bow shock wave will lie close to the surface of the body. The procedure for determining flow conditions in such flow fields is analogous to that employed in reference 1 for the case of axially symmetric flow fields; namely, the flow field is studied in two parts - flow at the vertex and flow downstream of the vertex. The combined results of these two phases of the investigation will then be applied to the determination of the whole flow field and, in particular, to the determination of flow properties on the body surface and the resulting shock-wave shape.

## Flow at the Vertex of a Lifting Body

It follows from the assumptions basic to this analysis that the flow at the vertex will be the same as for a cone tangent to the body at the vertex and immersed in the same free stream. All derivatives with respect to radial distance vanish for these conditions, and the equations of motion and continuity in spherical polar coordinates become (a schematic diagram of the polar coordinate system is shown in fig. 1)

$$v \frac{\partial u}{\partial \omega} + \frac{w}{\sin \omega} \frac{\partial u}{\partial \phi} - v^2 - w^2 = 0 \quad (1a)$$

$$v \frac{\partial v}{\partial \omega} + \frac{w}{\sin \omega} \frac{\partial v}{\partial \phi} + \frac{1}{\rho} \frac{\partial p}{\partial \omega} + uv - w^2 \cot \omega = 0 \quad (1b)$$

$$v \frac{\partial w}{\partial \omega} + \frac{w}{\sin \omega} \frac{\partial w}{\partial \phi} + \frac{1}{\rho \sin \omega} \frac{\partial p}{\partial \phi} + uw + vw \cot \omega = 0 \quad (1c)$$

and

$$2\rho u \sin \omega + v \sin \omega \frac{\partial \rho}{\partial \omega} + \rho \sin \omega \frac{\partial v}{\partial \omega} + v\rho \cos \omega + w \frac{\partial \rho}{\partial \phi} + \rho \frac{\partial w}{\partial \phi} = 0 \quad (2)$$

respectively. Since the total energy in the flow is constant, the following relations must be satisfied:

$$\frac{\gamma}{\gamma - 1} \left( \frac{1}{\rho} \frac{\partial p}{\partial \phi} - \frac{p}{\rho^2} \frac{\partial \rho}{\partial \phi} \right) = - \left( u \frac{\partial u}{\partial \phi} + v \frac{\partial v}{\partial \phi} + w \frac{\partial w}{\partial \phi} \right)$$

$$\frac{\gamma}{\gamma - 1} \left( \frac{1}{\rho} \frac{\partial p}{\partial \omega} - \frac{p}{\rho^2} \frac{\partial \rho}{\partial \omega} \right) = - \left( u \frac{\partial u}{\partial \omega} + v \frac{\partial v}{\partial \omega} + w \frac{\partial w}{\partial \omega} \right) \quad (3)$$

The entropy at any point in the flow may be expressed as

$$E - E_0 = \frac{R}{\gamma - 1} \ln \left[ \frac{p}{p_0} \left( \frac{\rho_0}{\rho} \right)^\gamma \right] \quad (4)$$

Equations (1), (2), and (3) together with the relation

$$a^2 = \frac{\gamma - 1}{2} (\hat{v}^2 - v^2)$$

may be combined (by eliminating the pressure and density terms) to obtain the general equation of motion

$$\frac{\gamma - 1}{2} (\hat{V}^2 - V^2) \left( 2u + v \cot \omega + \frac{\partial v}{\partial \omega} + \frac{1}{\sin \omega} \frac{\partial w}{\partial \phi} \right) - uv^2 - uw^2 -$$

$$v^2 \frac{\partial v}{\partial \omega} - \frac{w^2}{\sin \omega} \frac{\partial w}{\partial \phi} - \frac{vw}{\sin \omega} \frac{\partial v}{\partial \phi} - vw \frac{\partial w}{\partial \omega} = 0 \quad (5)$$

which, when combined with the appropriate shock-wave relations, defines the flow about a circular cone immersed at an angle of attack in a supersonic stream.

Conditions at the shock wave.- In order to obtain algebraic solutions for flow at the vertex, it is necessary to make some simplifying assumptions regarding the flow field. To this end, the conical shock is assumed to be circular but inclined at an angle  $\epsilon$  to the free stream.<sup>1</sup> Then, the angular difference between the cone axis and the shock axis is

$$\eta = \alpha - \epsilon \quad (6)$$

Now, the shock-wave angle measured from the cone axis,  $\omega_s$ , is referred to the free-stream direction by  $\omega_s + \alpha \cos \phi$ . The shock-wave angle measured from the shock axis,  $(\omega_s)_{\phi=0} + \eta$ , is referred to the free-stream direction by  $(\omega_s)_{\phi=0} + \eta + \epsilon \cos \phi$ . Hence,

$$\omega_s + \alpha \cos \phi = (\omega_s)_{\phi=0} + \eta + \epsilon \cos \phi$$

and by virtue of expression (6) the resulting equation for the shock angle may be written<sup>2</sup>

$$\omega_s = (\omega_s)_{\phi=0} + \eta(1 - \cos \phi) \quad (7)$$

where  $(\omega_s)_{\phi=0}$  is the shock angle in the plane of symmetry on the windward

---

<sup>1</sup>Experimental results indicate (as will be shown later) that for small angles of attack the conical shock does, in fact, remain nearly circular. Other investigators (notably Stone, see, e.g., ref. 6) have made a similar assumption. It should be noted, however, that the additional assumption commonly employed, namely, that the conical-shock apex angle is the same as in the nonyaw case, is not made here.

<sup>2</sup>It should be noted that all angles are measured with respect to the body axis. The procedure of developing all pertinent expressions in the body coordinate system will be employed throughout the analysis.

---

side of the cone (see fig. 1). Similarly, the meridian angle  $\varphi_s$ , measured with respect to the shock axis, may be related to the meridian angle  $\varphi$ , measured with respect to the cone axis, by

$$\sin \varphi_s = \sin \varphi (1 - \eta \cot \omega \cos \varphi)$$

and

$$\cos \varphi_s = \cos \varphi + \eta \cot \omega \sin^2 \varphi$$

The shape of the conical shock having been specified, the velocity components at the shock may be obtained from the oblique-shock-wave relations

$$u_s = V_o \cos[\omega_s + \alpha(\cos \varphi + \eta \cot \omega_s \sin^2 \varphi)] \quad (8)$$

$$w_s = V_o \sin \varphi (1 - \eta \cot \omega_s \cos \varphi) \quad (9)$$

$$\frac{v_s}{\hat{V}} = - \frac{\gamma - 1}{\gamma + 1} \frac{1 - \left(\frac{u_s}{\hat{V}}\right)^2 - \left(\frac{w_s}{\hat{V}}\right)^2}{\frac{V_o}{\hat{V}} \sin[\omega_s + \alpha(\cos \varphi + \eta \cot \omega_s \sin^2 \varphi)]} \quad (10)$$

If the shock angles in the plane of symmetry were known, flow conditions around the entire shock could be determined since the shock-wave angle in any plane could be determined from equation (7). In order to determine these shock-wave angles, it is necessary to determine the crossflow component of velocity,  $w$ , throughout the flow field. Attention is therefore turned in this direction.

Determination of crossflow component of velocity.— Recalling the basic assumption to this analysis, namely, that flow fields of the type under consideration are characterized by the bow shock lying close to the surface of the body (i.e.,  $\omega - \delta \ll 1$ ), it is reasoned that the variation of  $w$  with  $\omega$  should be small and it is assumed that

$$w = w_1(\omega) w_2(\varphi) \quad (11)$$

Now  $w_2(\varphi)$  is given by equation (9). There remains, then, the determination of  $w_1(\omega)$  in any meridian plane. To this end, consider equation (1a). Differentiating this equation twice with respect to  $\varphi$  and once with respect to  $\omega$  yields, in the plane of symmetry,

$$\left(\frac{\partial^2 v}{\partial \phi^2}\right)_{\phi=0} = \sin \omega \left(\frac{\partial^2 w}{\partial \phi \partial \omega} + \frac{\partial w}{\partial \phi} \cot \omega\right) \quad (12)$$

Now, if we let

$$\frac{\partial^2 v}{\partial \phi^2} = F(\omega) \quad (13)$$

equation (12) becomes, upon integration with respect to  $\omega$ ,

$$\frac{\partial w}{\partial \phi} \sin \omega = \left(\frac{\partial w}{\partial \phi}\right)_S \sin \omega_S - \int_{\omega}^{\omega_S} F(\omega) d\omega \quad (14)$$

Consider now the integral term in the above equation. At the surface of the body ( $v \equiv 0$ )

$$F(\omega) = 0$$

Since it seems reasonable that  $F(\omega)$  will be a monotonic function between the surface and the shock wave, it is assumed that this function will attain its maximum value at the shock and may be written (from eqs. (8), (9), (10), and (13))

$$F(\omega)_S = \frac{2(\gamma - 1)}{\gamma + 1} \left[ V_0 \cos(\omega_S + \alpha) (\epsilon - 2\alpha \eta \cot \omega_S) + \frac{(V_0 \epsilon) M_0 \epsilon}{M_0 \sin(\omega_S + \alpha)} \right] -$$

$$\frac{\gamma - 1}{\gamma + 1} \left[ 1 + \frac{1}{\frac{\gamma - 1}{2} M_0^2 \sin^2(\omega_S + \alpha)} \right] (\epsilon - 2\alpha \eta \cot \omega_S) V_0 \cos(\omega_S + \alpha)$$

Now, according to the above expression,  $F(\omega)$  is a maximum when  $M_0 \sin(\omega_S + \alpha)$  is a minimum. Since  $M_0 \sin(\omega_S + \alpha) \geq 1$  for attached shock waves, the maximum value of  $F(\omega)$  can be determined by setting  $M_0 \sin(\omega_S + \alpha)$  equal to 1 in the above expression. Hence, since  $M_0 \epsilon \sim 1$ , there results

$$F(\omega) < \frac{2(\gamma - 1)}{\gamma + 1} V_0 \epsilon - \frac{3 - \gamma}{\gamma + 1} V_0 \cos(\omega_S + \alpha) (\epsilon - 2\alpha \eta \cot \omega_S)$$

Hence,

$$|F(\omega)| < \epsilon$$

and it follows that

$$\int_{\omega}^{\omega_S} F(\omega) d\omega < \int_{\omega_C}^{\omega_S} \epsilon d\omega = \epsilon(\omega_S - \omega_C)$$

Therefore the integral term in equation (14) is, at most, second order and can be neglected in this analysis. Equation (14) now can be written

$$\frac{\partial w}{\partial \phi} = \left( \frac{\partial w}{\partial \phi} \right)_S \frac{\sin \omega_S}{\sin \omega}$$

Hence,

$$w_1(\omega) = \frac{\sin \omega_S}{\sin \omega}$$

and it appears that expression (11) is a logical assumption since the variation of  $w$  with  $\omega$  is, in fact, small. Combination of the above expression with equations (9) and (11) yields, then,

$$w = V_0 \epsilon \frac{\sin \omega_S}{\sin \omega} \sin \phi (1 - \eta \cot \omega_S \cos \phi) \quad (15)$$

defining the crossflow component of the velocity anywhere in the flow field relative to the cone axis.

Having determined an expression for  $w$  throughout the flow field, one can now obtain a solution to the flow in the plane of symmetry in a manner analogous to that presented in reference 1 for the case of axially symmetric conical flows. Since the calculation of the flow in this plane requires simultaneous solutions of the conical flow equations and the oblique shock-wave relations, the procedure is somewhat involved and, hence, is given in Appendix A. After  $(\omega_S)_{\phi=0}$  and  $\epsilon$  have been determined from Appendix A, conditions around the entire shock front can be determined from equations (6) through (10). Determination of flow conditions around the cone surface will now be considered.

Flow conditions on the surface. - It has been shown by Ferri in reference 7 that to the first order in  $\alpha$  the entropy remains constant in a meridian plane (having the value that exists at the shock in that plane) until a vortical layer is reached at the surface of the body across which a variation of entropy occurs. Since the entropy on the surface is

constant, it must have the same value that exists in the plane  $\phi = 0$ . Now the thickness of the vortical layer being of the order of  $\alpha^2$ , the pressure remains constant through the layer to the first order of  $\alpha$  and the component of velocity normal to the surface can be considered zero on the external side of the layer. Hence, across this vortical layer

$$p_c = p_e$$

$$v_c = v_e = 0$$

and

$$E_c = (E)_{\phi=0}$$

where the subscripts  $c$  and  $e$  refer to quantities inside and outside the layer, respectively. Consider now an expression relating  $u$  and  $w$  on the surface of the cone which may be obtained from equation (1a); namely,

$$\frac{\partial u}{\partial \phi} = w \sin \delta_c$$

or

$$u = (V_c)_{\phi=0} + \sin \delta_c \int_0^\phi w \, d\phi \quad (16)$$

Since the thickness of the vortical layer is proportional to  $\alpha^2$ , the normal component of the velocity is zero through the layer and the above expression holds on either side of the vortical layer. An expression for the velocity and, hence, the Mach number externally adjacent to the vortical layer may then be easily determined as follows. The expression for the crossflow at the vortical layer may be written in the form (from eq. (15))

$$\frac{w_e}{(V_c)_{\phi=0}} = \frac{V_o}{(V_c)_{\phi=0}} \epsilon \frac{\sin \omega_s}{\sin \delta_c} \sin \phi (1 - \eta \cot \omega_s \cos \phi) \quad (17)$$

Substituting this expression in equation (16) yields, upon integration,

$$\frac{u_e}{(V_c)_{\phi=0}} = 1 + \frac{V_o}{(V_c)_{\phi=0}} \epsilon \sin \omega_s \left( 1 - \cos \phi - \frac{\eta}{2} \cot \omega_s \sin^2 \phi \right) \quad (18)$$

The Mach number at the external side of the vortical layer,  $M_e$ , may be determined from the relation

$$M_e^2 = \frac{(M_c)_{\varphi=0}^2 \left[ \frac{V_e}{(V_c)_{\varphi=0}} \right]^2}{1 - \frac{\gamma - 1}{2} (M_c)_{\varphi=0}^2 \left\{ \left[ \frac{V_e}{(V_c)_{\varphi=0}} \right]^2 - 1 \right\}} \quad (19)$$

where, of course,

$$\left[ \frac{V_e}{(V_c)_{\varphi=0}} \right]^2 = \frac{u_e^2 + w_e^2}{(V_c)_{\varphi=0}^2}$$

The velocity and the Mach number in the  $\varphi = 0$  plane are given by (see Appendix A)

$$\left( \frac{V}{V_s} \right)_{\varphi=0} = \left\{ \frac{\cos(\omega_s - \delta_s)}{\cos \left[ \frac{(\delta_c - \delta)(\omega_s - \delta_s)}{\delta_c - \delta_s} \right]} \right\}^{\frac{\delta_c - \delta_s}{\omega_s - \delta_s}}$$

and

$$(M)_{\varphi=0}^2 = \frac{(M_s)_{\varphi=0}^2 \left( \frac{V}{V_s} \right)_{\varphi=0}^2}{1 - \frac{\gamma - 1}{2} (M_s)_{\varphi=0}^2 \left[ \left( \frac{V}{V_s} \right)_{\varphi=0}^2 - 1 \right]}$$

respectively, where

$$(M_s)_{\varphi=0}^2 = \frac{(\gamma + 1)^2 M_o^4 \sin^2[(\omega_s)_{\varphi=0} + \alpha] - 4 \left\{ M_o^2 \sin^2[(\omega_s)_{\varphi=0} + \alpha] - 1 \right\} \left\{ \gamma M_o^2 \sin^2[(\omega_s)_{\varphi=0} + \alpha] + 1 \right\}}{\left\{ 2\gamma M_o^2 \sin^2[(\omega_s)_{\varphi=0} + \alpha] - (\gamma - 1) \right\} \left\{ (\gamma - 1) M_o^2 \sin^2[(\omega_s)_{\varphi=0} + \alpha] + 2 \right\}}$$

If one employs the condition that the pressure is constant across the vortical layer, an expression defining the Mach number directly on the surface of the body,  $M_c$ , in terms of the Mach number at the vortical layer, may be obtained; namely,

$$M_c^2 = \left( \frac{2}{\gamma - 1} + M_e^2 \right) e^{\frac{E_e - E_c}{\gamma C_v}} - \frac{2}{\gamma - 1} \quad (20)$$

where (since  $E_c = (E)_{\varphi=0}$ )

$$\frac{E_e - E_c}{\gamma C_v} = \frac{\left( M_o^2 \sin^2[(\omega_s)_{\varphi=0} + \alpha] \left\{ (\gamma - 1) M_o^2 \sin^2[\omega_s + \alpha(\cos \varphi + \eta \cot \omega_s \sin^2 \varphi)] + 2 \right\} \right)}{\left( M_o^2 \sin^2[\omega_s + \alpha(\cos \varphi + \eta \cot \omega_s \sin^2 \varphi)] \left\{ (\gamma - 1) M_o^2 \sin^2[(\omega_s)_{\varphi=0} + \alpha] + 2 \right\} \right)}$$

$$\left\{ \frac{2\gamma M_o^2 \sin^2[\omega_s + \alpha(\cos \varphi + \eta \cot \omega_s \sin^2 \varphi)] - (\gamma - 1)}{2\gamma M_o^2 \sin^2[(\omega_s)_{\varphi=0} + \alpha] - (\gamma - 1)} \right\}^{\frac{1}{\gamma}} \quad (21)$$

Since the flow is isentropic in the  $\varphi = 0$  plane (downstream of the shock wave) and around the surface of the body inside the vortical layer, the pressure coefficient anywhere on the surface may, of course, be obtained by the expression

$$P_c = \frac{2}{\gamma M_o^2} \left[ \frac{(p_s)_{\phi=0}}{p_o} \frac{p}{(p_s)_{\phi=0}} - 1 \right] \quad (22)$$

where

$$\frac{(p_s)_{\phi=0}}{p_o} = \frac{2\gamma M_o^2 \sin^2 \left[ (\omega_s)_{\phi=0} + \alpha \right] - (\gamma - 1)}{\gamma + 1}$$

$$\frac{p}{(p_s)_{\phi=0}} = \left[ \frac{1 + \frac{\gamma - 1}{2} (M_s)_{\phi=0}^2}{1 + \frac{\gamma - 1}{2} M^2} \right]^{\frac{\gamma}{\gamma - 1}}$$

and  $M^2$  is given by equation (20).

Flow conditions off the surface.- Flow conditions in the plane of symmetry, on the surface of the cone, and at the conical shock having been determined, the flow throughout the remainder of the flow field may now be calculated. Since only high Mach number flows are considered in this analysis, the variation of the magnitude of the resultant velocity in a meridian plane will be small. Hence, the variation of  $u$  and  $v$  will be small and may be represented by a power series in  $(\omega - \delta_c)$  where the coefficients are determined by the requirements

$$u = u_e \quad \text{at} \quad \omega = \delta_c$$

$$u = u_s \quad \text{at} \quad \omega = \omega_s$$

$$\frac{\partial u}{\partial \omega} = \left( \frac{\partial u}{\partial \omega} \right)_e \quad \text{at} \quad \omega = \delta_c$$

and

$$v = 0 \quad \text{at} \quad \omega = \delta_c$$

$$v = v_s \quad \text{at} \quad \omega = \omega_s$$

$$\frac{\partial v}{\partial \omega} = \left( \frac{\partial v}{\partial \omega} \right)_e \quad \text{at} \quad \omega = \delta_c$$

Thus,

$$u = u_e + \left(\frac{\partial u}{\partial \omega}\right)_e (\omega - \delta_c) \left(\frac{\omega_s - \omega}{\omega_s - \delta_c}\right) + (u_s - u_e) \left(\frac{\omega - \delta_c}{\omega_s - \delta_c}\right)^2 \quad (23)$$

and

$$v = \left(\frac{\partial v}{\partial \omega}\right)_e (\omega - \delta_c) \left(\frac{\omega_s - \omega}{\omega_s - \delta_c}\right) + v_s \left(\frac{\omega - \delta_c}{\omega_s - \delta_c}\right)^2 \quad (24)$$

where  $\omega_s$ ,  $u_s$ ,  $v_s$ , and  $u_e$  are given by equations (7), (8), (10), and (18), respectively. There remains now the determination of  $(\partial u / \partial \omega)_e$  and  $(\partial v / \partial \omega)_e$ . To this end, consider equation (1b). Just outside the vortical layer this equation reduces to

$$\left(\frac{1}{\rho} \frac{\partial p}{\partial \omega}\right)_e = w_e^2 \cot \delta_c \quad (25)$$

It will be recalled that the entropy was assumed constant between the shock and the vortical layer in each meridian plane. Now Euler's equation for compressible flow along a stream tube may be written ( $\varphi = \text{constant}$ )

$$\frac{1}{\rho} \frac{\partial p}{\partial \omega} = -v \frac{\partial v}{\partial \omega}$$

Combination of this expression with equation (25) yields

$$\left(v \frac{\partial v}{\partial \omega}\right)_e = -w_e^2 \cot \delta_c$$

from which may be obtained (noting that at the surface  $v^2 = u^2 + w^2$ )

$$\left(\frac{\partial u}{\partial \omega}\right)_e = \left(\frac{w}{u}\right)_e \left[\left(\frac{\partial w}{\partial \omega}\right)_e + w_e \cot \delta_c\right] \quad (26)$$

where  $w_e$  is given by equation (17) and

$$\left(\frac{\partial w}{\partial \omega}\right)_e = -V_o \epsilon \frac{\sin \omega_s}{\sin \delta_c} \cot \delta_c \sin \varphi (1 - \eta \cot \omega_s \cos \varphi) \quad (27)$$

Now from equation (5) there results (setting  $v = 0$ )

$$\left(\frac{\partial v}{\partial \omega}\right)_e = \left[u_e + \csc \delta_c \left(\frac{\partial w}{\partial \varphi}\right)_e\right] \left[M_e^2 \left(\frac{w_e}{V_e}\right)^2 - 1\right] - u_e \quad (28)$$

where  $M_e$  is known from equation (19) and from equation (15)

$$\left(\frac{\partial w}{\partial \varphi}\right)_e = V_{0e} \frac{\sin \omega_s}{\sin \delta_c} (\cos \varphi - \eta \cot \omega_s \cos 2\varphi) \quad (29)$$

The components of the local velocity anywhere in the flow field external to the vortical layer are now known from equations (15), (23), and (24). Hence, the magnitude and direction of the resultant velocity and, consequently, the Mach number may easily be determined. If the Mach number is known, the local pressure (in coefficient form) may be obtained anywhere in the flow field with the aid of the expression

$$P = \frac{2}{\gamma M_0^2} \left( \frac{p_s}{p_0} \frac{p}{p_s} - 1 \right) \quad (30)$$

where

$$\frac{p_s}{p_0} = \frac{2\gamma M_0^2 \sin^2[\omega_s + \alpha(\cos \varphi + \eta \cot \omega_s \sin^2 \varphi)] - (\gamma - 1)}{\gamma + 1} \quad (31)$$

and, of course,

$$\frac{p}{p_s} = \left( \frac{1 + \frac{\gamma - 1}{2} M_s^2}{1 + \frac{\gamma - 1}{2} M^2} \right)^{\frac{\gamma}{\gamma - 1}} \quad (32)$$

The Mach number and pressure distribution (as well as the orientation of the conical shock) are now known throughout the flow field around a lifting circular cone.

The range of applicability of the results of this analysis is considered to be the same as that of the nonlifting cone solutions presented in reference 1. This results from the fact that when  $\alpha = 0$ , equation (A7) in Appendix A reduces identically to the equation defining the deflection angle in reference 1. As was pointed out in this reference, when

$M_S(\omega_S - \delta_C) > 1/2$  an imaginary value of  $\delta_S$  is obtained. If  $\alpha > 0$ , equation (A7) yields a real value of  $\delta_S$ , (for  $M_S(\omega_S - \delta_C) > 1/2$ ), however, it would not be expected that the range of applicability of this equation (in terms of  $M_0$  and  $\delta_C$ ) would be increased for finite  $\alpha$ . Figure 2 shows the boundary line (given by  $M_S(\omega_S - \delta_C) = 1/2$  for  $\alpha = 0$ ) above which the present conical flow solutions are applicable. The dashed line represents the boundary below which the results of Stone's second-order solution (ref. 5) are available.

The flow around circular cones traveling at small angles of attack and at high supersonic airspeeds can be calculated by means of the foregoing algebraic expressions. As was pointed out previously, these expressions can be employed to determine fluid properties at the vertices of pointed bodies of revolution other than cones. Investigation of flow downstream of the vertices of such bodies is now undertaken.

#### Flow Downstream of the Vertex

In this study we exploit the finding of reference 3 that many three-dimensional hypersonic flows may be treated by a generalized shock-expansion method which is analogous to that employed in reference 4 for two-dimensional flows. Specifically, this treatment is permissible when disturbances associated with the divergence of streamlines in planes tangent to a surface can be considered negligible compared to those associated with the curvature of streamlines in planes normal to the surface. For the case of noninclined bodies of revolution which are curved in the stream direction, this requirement is satisfied when the hypersonic similarity parameter is greater than about 1 (see ref. 1). For inclined bodies, an additional restriction is imposed. This point is perhaps best clarified by considering the problem of calculating flow at the surface.

It follows from reference 3 that when the generalized shock-expansion method applies in the region downstream of the vertex, surface streamlines can be approximated by geodesic lines. The only geodesics on the surface of a body of revolution which, like streamlines, do not intersect each other are the meridian lines. In addition, the meridian lines are the only geodesics which, like the streamlines, pass through the vertex. When the shock-expansion method is applied, then, surface streamlines are approximated by meridian lines. Strictly speaking, however, this can be the case only when  $\alpha \ll 1$ . (It should be noted that this is always true, independent of  $\alpha$ , for the extreme windward and leeward streamlines.) Evidently, then, the generalized shock-expansion method should be applicable to curved bodies of revolution only at small angles of attack in flows characterized by a value of the hypersonic similarity parameter greater than about 1.

The procedure for determining flow conditions at the surface of a lifting body is entirely analogous to that employed in the application of the shock-expansion method to the nonlifting body (ref. 1). For example, the Mach number on the surface at the vertex is obtained with the aid of equation (20). The variation of Mach number downstream of the vertex is then obtained by means of the isentropic expansion relation (see ref. 1)

$$\delta_B - \delta_A = \sin^{-1} \frac{1}{M_A} - \sin^{-1} \frac{1}{M_B} +$$

$$\sqrt{\frac{\gamma+1}{\gamma-1}} \left[ \tan^{-1} \sqrt{\frac{\gamma+1}{(\gamma-1)(M_B^2-1)}} - \tan^{-1} \sqrt{\frac{\gamma+1}{(\gamma-1)(M_A^2-1)}} \right] \quad (33)$$

where A and B are different points on the same meridian line (or streamline). If the Mach number distribution is known, the pressure distribution (in coefficient form) on the surface is readily obtained with the aid of equation (22). It should be noticed that when  $M_c$  is employed, equation (33) yields the Mach number distribution on the body under the vortical layer.<sup>3</sup> This result materially reduces the net labor associated with carrying out the calculations to determine the pressure distributions around the body downstream of the vertex since the pressure rise across the shock need be considered only in the plane  $\phi = 0$  (see eq. (22)). It results, too, that a relatively simple expression for  $\left. \frac{dC_N}{d\alpha} \right|_{\alpha=0}$ , the initial slope of the normal-force-coefficient curve, can be obtained. The development of this expression follows.

The expression for the normal-force coefficient on a body of revolution may be written

$$C_N = \frac{16}{\gamma M_o^2 \pi d^2} \int_0^l \int_0^\pi \frac{p}{p_o} r \cos \phi \, d\phi \, dx \quad (34)$$

where  $d$  is the diameter of the base and  $r$  is the local radius of the body. Differentiating expression (34) with respect to  $\alpha$  and employing the condition of constant entropy on the surface results in

---

<sup>3</sup>It is reasoned that since a vortical layer exists around the body surface at the vertex, then a vortical layer must exist downstream of the vertex as well.

---

$$\left. \frac{dC_N}{d\alpha} \right|_{\alpha=0} = \frac{16}{\gamma M_0^2 \pi d^2} \int_0^l \int_0^\pi \left( \frac{p}{p_N} \right) \frac{\sin 2\beta_N}{\sin 2\beta} \frac{d}{d\alpha} \left( \frac{p_N}{p_0} \right) r \cos \varphi \, d\varphi \, dx \quad (35)$$

This expression may be rewritten in terms of the initial normal-force-curve slope for a cone tangent to the body at the vertex; namely,

$$\left. \frac{dC_N}{d\alpha} \right|_{\alpha=0} = 8 \left( \frac{l}{d} \right)^2 \left. \frac{dC_N}{d\alpha} \right|_{TCN} \tan \delta_N \int_0^1 \left( \frac{p}{p_N} \right) \left( \frac{\sin 2\beta_N}{\sin 2\beta} \right) \left( \frac{r}{l} \right) d \left( \frac{x}{l} \right) \quad (36)$$

where the subscript TCN refers to a cone tangent at the vertex. The calculations necessary to determine the initial normal-force-curve slope for a body of revolution are relatively simple, since  $\left. \frac{dC_N}{d\alpha} \right|_{TCN}$  may easily be obtained from Stone's first-order theory (ref. 6) or from chart 8 in reference 8. The Mach number and pressure distribution along the body may be obtained by the conical shock-expansion method presented in reference 1.<sup>4</sup> Having determined these distributions, one may easily evaluate the integral term in equation (36) by numerical integration or by graphical methods.

In order to determine fluid properties in the flow field other than on the surface, it is necessary to know flow conditions just outside the vortical layer downstream of the vertex. These conditions may be determined in the same manner as before except that now initial flow conditions externally adjacent to the vortical layer at the vertex are employed. For example, the Mach number at the vertex is determined by means of equation (19). Equation (33) is then employed, as before, to obtain the Mach number distribution downstream of the vertex. When flow conditions along this layer in a meridian plane have been established, fluid properties throughout the plane may be calculated after the manner described in reference 4. Application of the generalized-shock-expansion method for determining the flow field in any meridian plane is discussed in Appendix B.

#### Simplified Expressions for Slender Lifting Bodies

In the case of slender bodies traveling at very high Mach numbers (again  $\alpha \ll 1$ ) the calculations of fluid properties at the surface become relatively simple and, hence, merit special attention. As in the case of the nonlifting body, a hypersonic slender-body theory yielding

---

<sup>4</sup>It is clear that the shock-expansion method discussed previously in the present paper may also be used since the expressions developed herein reduce identically to those of reference 1 when  $\alpha = 0$ .

explicit solutions for the Mach number and pressure at any point on the surface of the body can be obtained. These solutions may be summarized (from Appendix C) as follows. The local Mach number at any point is given by the relation

$$M = \frac{M_N}{1 - \frac{\gamma - 1}{2} (M_N \delta_N) \left(1 - \frac{\delta}{\delta_N}\right)} \quad (37)$$

where

$$M_N^2 = \frac{(M_S)_{\varphi=0}^2 \left\{ 1 + \frac{\gamma - 1}{2} (M_S \delta_N)^2 \left[ 1 + \ln \left( \frac{\delta_N}{\omega_S} \right)^2 - \left( \frac{\delta_S}{\delta_N} \right)^2 - 2 \left( \frac{\epsilon}{\delta_N} \right) \left( \frac{\omega_S}{\delta_N} - 1 \right) \right] \right\}_{\varphi=0}}{\frac{E_c - E_e}{e^{\gamma C_V}} \left\{ 1 - \frac{\gamma - 1}{2} (M_N \epsilon)_{\varphi=0}^2 \left[ \frac{2\omega_S}{\epsilon} (1 - \cos \varphi) + \left( \frac{\omega_S}{\delta_N} \right)^2 \sin^2 \varphi \right] \right\}}$$

and

$$\left( \frac{\delta_S}{\delta_N} \right)_{\varphi=0}^2 = \left[ \frac{\delta_N}{\omega_S} - \frac{\epsilon}{\omega_S} \left( \frac{\omega_S}{\delta_N} - 1 \right) \right]_{\varphi=0}^2$$

$$(M_S)_{\varphi=0}^2 = \frac{(\gamma + 1)^2 M_O^4 \left[ (\omega_S)_{\varphi=0} + \alpha \right]^2}{\left\{ 2\gamma M_O^2 \left[ (\omega_S)_{\varphi=0} + \alpha \right]^2 - (\gamma - 1) \right\} \left\{ (\gamma - 1) M_O^2 \left[ (\omega_S)_{\varphi=0} + \alpha \right]^2 + 2 \right\}}$$

$$\frac{E_c - E_e}{e^{\gamma C_V}} = \left\{ \frac{2\gamma M_O^2 \left[ (\omega_S)_{\varphi=0} + \alpha \right]^2 - (\gamma - 1)}{2\gamma M_O^2 (\omega_S + \alpha \cos \varphi)^2 - (\gamma - 1)} \right\}^{\frac{1}{\gamma}} \left( \frac{M_O^2 (\omega_S + \alpha \cos \varphi)^2 \left\{ (\gamma - 1) M_O^2 \left[ (\omega_S)_{\varphi=0} + \alpha \right]^2 + 2 \right\}}{M_O^2 \left[ (\omega_S)_{\varphi=0} + \alpha \right]^2 \left[ (\gamma - 1) M_O^2 (\omega_S + \alpha \cos \varphi)^2 + 2 \right]} \right)$$

Unless otherwise designated,  $\omega_S$  in the above expressions is given by

$$\omega_S = (\omega_S)_{\varphi=0} + \eta(1 - \cos \varphi)$$

and  $(\omega_s)_{\phi=0}$  is determined from equation (C7) in Appendix C. Now

$$\eta = \frac{1 - \frac{\gamma+1}{4} \frac{\delta_s}{\delta_N} \left(1 + \frac{\delta_s}{\delta_N}\right)}{1 + \frac{\gamma+1}{4} \left(1 - \frac{\delta_s}{\delta_N}\right)} \alpha$$

where

$$\frac{\delta_s}{\delta_N} = \frac{M_0 \delta_N}{\sqrt{1 + \frac{\gamma+1}{2} (M_0 \delta_N)^2}}$$

and, of course,

$$\epsilon = \alpha - \eta$$

The pressure coefficient at any point on the surface may be obtained from the expression

$$P = \frac{2}{\gamma M_0^2} \left\{ \left( \frac{p_s}{p_0} \right)_{\phi=0} \left[ \frac{(M_s)_{\phi=0}}{M_N} - \frac{\gamma-1}{2} (M_s \delta_N)_{\phi=0} \left( 1 - \frac{\delta}{\delta_N} \right) \right]^{\frac{2\gamma}{\gamma-1}} - 1 \right\} \quad (38)$$

It is interesting to note that equations (37) and (38) predict the ratios of local to free-stream Mach numbers, and local to free-stream static pressures to be the same at corresponding points on related bodies, provided that the flow fields about these bodies are related by the same respective values of the hypersonic similarity parameters  $M_0 \delta_N$  and  $M_0 \alpha$ . These predictions<sup>5</sup> are identical to those of reference 9 for inviscid flow about slender three-dimensional shapes. Hence, these expressions readily lend themselves to solutions in terms of  $M_0 \delta_N$  and  $M_0 \alpha$  in tabular form. Calculations over a range of  $M_0 \delta_N$  from 0.6 to 3.0 and  $\alpha/\delta_N$  from 0 to 1 were carried out for flow at the vertex of a body of revolution and the results of these calculations for the flow parameters

$\frac{(M_s)_{\phi=0}}{M_N}$ ,  $\frac{(p_s/p_0)_{\phi=0}}{(M_0 \delta_N)^2}$ , and  $(M_s \delta_N)_{\phi=0}$  are tabulated in table I for 30° increments of  $\phi$  from 0° to 180°. Thus, for a given  $M_0 \delta_N$  and  $M_0 \alpha$ , the Mach number on the surface of a body downstream of the vertex is readily obtained with the aid of these tabulated parameters when used in conjunction with equation (37). The pressure coefficient anywhere on the surface of the body is easily calculated by means of equation (38).

---

<sup>5</sup>In the case where  $\alpha = 0$ , the expressions developed in the present paper reduce identically to those presented in reference 1.

The results from table I may also be used to good advantage in determining the initial normal-force-curve slopes for slender bodies of revolution. For example, from Appendix C there is obtained

$$\left. \frac{dC_N}{d\alpha} \right|_{\alpha=0} = 8 \left( \frac{l}{d} \right)^2 \delta_N \left. \frac{dC_N}{d\alpha} \right|_{TCN} \int_0^1 \left[ 1 - \frac{\gamma-1}{2} (M_N \delta_N) \left( 1 - \frac{\delta}{\delta_N} \right) \right]^{\frac{\gamma+1}{\gamma-1}} \left( \frac{r}{l} \right) d \left( \frac{x}{l} \right) \quad (39)$$

where

$$\left. \frac{dC_N}{d\alpha} \right|_{TCN} = \frac{\left( \frac{M_s}{M_N} \right)^{\frac{2\gamma}{\gamma-1}} \left[ 1 + \frac{\gamma+3}{2} (M_O \delta_N)^2 \right] \left\{ \left[ 1 + \frac{\gamma-1}{2} (M_O \delta_N)^2 \right] \left[ 1 + \gamma (M_O \delta_N)^2 \right] \left( \frac{M_N}{M_O} \right)^2 - \left( \frac{\delta_s}{\delta_N} \right)^2 (M_O \delta_N)^2 \right\}}{(M_O \delta_N)^2 \left[ \frac{\gamma+5}{\gamma+1} \left( \frac{\delta_N}{\delta_s} \right) - 1 \right] \left[ 1 + \frac{\gamma-1}{2} (M_O \delta_N)^2 \right]}$$

Hence, the pertinent flow parameters necessary to determine the initial slope of the normal-force-coefficient curve by means of the above expressions may be obtained from table I for the case of  $\alpha/\delta_N = 0$ .

## EXPERIMENT

In order to obtain a check on the predictions of the preceding theoretical analysis, the pressures acting on the surfaces of lifting bodies of revolution corresponding to values of the hypersonic similarity parameter  $K$  from 0.60 to 1.68 at Mach numbers from 3.00 to 5.05 were determined experimentally. The bodies were tested at angles of attack up to  $15^\circ$ . A brief description of these tests follows.

### Test Apparatus

Tests were conducted in the Ames 10- by 14-inch supersonic wind tunnel. A detailed description of the wind tunnel and auxiliary equipment may be found in reference 10. The pressures acting on the model surfaces were measured with a mercury U-tube manometer or by means of McCleod gages when the pressures were low enough to be recorded on the latter.

Pressure-distribution models were mounted on a  $0^\circ$  model support and on  $5^\circ$ ,  $10^\circ$ , and  $15^\circ$  bent supports. The test models were two tangent ogives

having fineness ratios 3 and 5 and two cones having the same vertex angles as the ogives. The dimensions of these models and location of the pressure orifices are shown in figure 3.

### Tests and Procedure

Pressures on the model surfaces were measured at  $0^\circ$ ,  $5^\circ$ ,  $10^\circ$ , and  $15^\circ$  angles of attack at test Mach numbers of 3.00, 4.25, and 5.05. The Reynolds numbers (based on maximum diameter of the ogives) were 1.09 million at Mach numbers 3.00 and 4.25, and 0.52 million at Mach number 5.05.

The pressures around the cone surface ( $0^\circ$  to  $360^\circ$ ) at meridian stations  $45^\circ$  apart were recorded simultaneously at each Mach number and angle of attack. In the case of the two ogival models, the pressures were recorded at meridian stations  $90^\circ$  apart. Each model was then rotated  $45^\circ$  about its longitudinal axis (except at  $0^\circ$  angle of attack) and the process repeated.

Schlieren photographs of the bow shock waves in three meridian planes were also obtained.

### Accuracy of Test Results

The variation in Mach number from the nominal value did not exceed  $\pm 0.02$  in the region of the test section where the models were located.

The precision of the computed pressure coefficients was affected by inaccuracies in the pressure measurements, as well as uncertainties in the stream angle and the free-stream dynamic pressure. The resulting errors in the pressure coefficients were generally less than  $\pm 0.005$  throughout the Mach number range for all angles of attack. The meridian angles at which the pressure coefficients are plotted are considered accurate to within  $\pm 1^\circ$ .

## COMPARISON OF THEORY WITH EXPERIMENT AND DISCUSSION OF RESULTS

### Flow at the Vertex

It will be recalled that one of the fundamental assumptions in the development of the conical flow theory was that the conical shock remains circular when the cone is inclined. It is appropriate to examine the validity of this assumption before proceeding with a comparison of the theoretical and experimental surface pressures. To this end, schlieren

evidence on the shapes of the conical shocks for the two test cones at Mach number 5.05 is presented in figures 4 and 5 for angles of attack of  $0^\circ$ ,  $5^\circ$ ,  $10^\circ$ , and  $15^\circ$ . The data shown in the figures were obtained by measuring the angle of the shock in the schlieren photographs at various meridian stations. Theory is compared with experiment in a cross-sectional plane at an arbitrary distance downstream of the vertex. It is observed in figure 4 that the conical shock attached to the slender cone remains nearly circular for angles of attack up to  $10^\circ$ . At  $\alpha = 15^\circ$ , the angle of attack is greater than the cone half-angle and, as might be expected, the shock is no longer circular. However, in the case of the blunt cone (fig. 5), the conical shock remains essentially circular for all angles of attack up to and including  $15^\circ$ . It would appear, then, that at least for moderate cone angles, so long as the angle of attack is less than the semivertex angle of the cone, the assumption of a circular conical shock made in the analysis is justified.

The second basic assumption employed in the development of the conical flow theory of this paper is that  $\omega - \delta \ll 1$ . It is apparent that this condition is best satisfied for blunt cones and for high Mach numbers. The accuracy of the theory might be expected, therefore, to improve both with increasing cone angle and increasing Mach number. The predictions of theory and the results of the pressure-distribution tests for the two test cones ( $\delta_c = 11.42^\circ$  and  $\delta_c = 18.92^\circ$ ) are shown in figures 6, 7, and 8. The data are plotted in the form of surface pressure coefficient as a function of the meridian angle  $\phi$ .<sup>6</sup> It is observed in these figures that the predictions of theory, when applicable, are in good agreement with experiment for the Mach numbers and angles of attack presented. It is evident also that at the highest angle of attack ( $\alpha = 15^\circ$ ) the theory is less reliable on the leeward side of the body. Although this result is due in part to the limitations of the theory, it is also clear that the viscous effects of the flow are influencing the pressures to a greater extent over the leeward portion of the body. It can also be deduced from these figures that agreement between theory and experiment is better for the blunter cone, particularly at the higher angles of attack. It is indicated, therefore, that the predictions of the conical flow theory of this paper will yield more reliable results when the parameter  $\alpha/\delta_c < 1$ . In the lower range of  $M_0$  and  $\delta_c$  (fig. 6) where the present conical flow theory is not applicable (see fig. 2), Stone's second-order solution (ref. 11) applied in the manner described in reference 12 yields results which are in good agreement with experiment.<sup>7</sup> It is observed in figure 7

<sup>6</sup>It will be noted in these and subsequent figures that the data are often plotted at meridian stations slightly different from  $0^\circ$ ,  $45^\circ$ ,  $90^\circ$ , etc. This resulted from inaccuracies in rotational positioning of the model.

<sup>7</sup>Due to the limited range of the results presented in the tables of reference 5, comparison can be made only for the slender cone and then only for Mach numbers 3.00 and 4.25 without resorting to extrapolation. Although the agreement between Stone's results and experiment appears to be better at  $\alpha = 10^\circ$  than at  $\alpha = 5^\circ$ , this result must be attributed to the manner in which the flow parameters presented in reference 5 were interpolated.

that both methods yield comparable results over the angle-of-attack range at Mach number 4.25. Hence, it appears that the two theories tend to overlap in regards to their usefulness over the range of  $M_0$  and  $\delta_c$ .

It should be mentioned here that the treatment of inclined cone flow as presented by Ferri in references 7 and 13 was applied to the cases under discussion in the present paper. Ferri's method did not yield results as good as either Stone's second-order theory (where applicable) or the conical flow theory of the present paper. In fact, inconsistent results were obtained when the method was applied according to references 7 and 13. This discrepancy may be traced to what appears to be an inconsistency between equation (55) in reference 7 and equation (55) in reference 13.

From the preceding comparisons of the experimentally determined surface pressures and shock-wave shapes with the predictions of the conical flow solutions of this paper, it is indicated that the latter solutions may be employed to predict the flow properties about a lifting cone at high supersonic airspeeds with good accuracy when the angle of attack is less than the cone half-angle (i.e., when  $\alpha/\delta_c < 1$ ). It is therefore suggested that these solutions may be particularly useful for determining conical flow fields about lifting cones over the range of  $M_0$  and  $\delta_c$  not treated in the M.I.T. tables (ref. 5).

#### Flow Downstream of the Vertex

It remains now to determine the accuracy with which the solutions for flow about lifting cones in combination with the isentropic expansion equations predict the flow about bodies of revolution other than cones. The pressure distributions on the surfaces of two ogives (having fineness ratios 3 and 5) at Mach numbers 3.00, 4.25, and 5.05 and at angles of attack of  $0^\circ$ ,  $5^\circ$ ,  $10^\circ$ , and  $15^\circ$  were calculated using the methods of this paper. These distributions are presented in figures 9, 10, and 11 for values of the hypersonic similarity parameter,  $K$ , varying from 0.60 to 1.68. Also shown are the results of the pressure-distribution tests for the two ogival models.

Comparing first the predictions of theory with experiment for the case of zero lift (fig. 9), we observe that the accuracy of the shock-expansion method generally improves with increasing  $K$ . This trend is, of course, the same as was observed in reference 1 for comparisons of the predictions of the shock-expansion method with those of the method of characteristics. The results of a characteristics solution for the  $l/d = 3$  ogive at  $M_0 = 3.00$  (from ref. 14) are also shown for comparative purposes. Characteristics solutions are not available for the other cases; however, the results of Rossow (which were obtained by correlating the pressures obtained by characteristics solutions according to the hypersonic similarity law and presented in ref. 15) are shown. As might be expected, Rossow's results are generally in good agreement with experiment although there is a slight underestimation of the pressures near the base of the

body at  $M_0 = 5.05$ . This is attributed to the viscous effects of the flow which are probably influencing the pressures at this Mach number. In any event, it is evident that the predictions of Rossow and the shock-expansion method are in good agreement at the highest value of  $K$  ( $K = 1.68$ ).

It is of interest now to determine the reliability of the predictions of the shock-expansion method for lifting bodies. As shown in figure 10, the theory yields good agreement with experiment for the fineness-ratio-5 ogive on the windward side of the body except at  $M_0 = 3.00$  ( $K = 0.60$ ).<sup>8</sup> Some disagreement is evident, however, on the leeward side of the body at all Mach numbers. In the case of the fineness-ratio-3 ogive (fig. 11), agreement is generally better over the entire body at each angle of attack, particularly at the higher values of  $K$  ( $K > 1$ ). It will be recalled from figure 9 that at  $\alpha = 0^\circ$  the longitudinal pressure distributions on both ogives indicated that the accuracy of the shock-expansion method increased as  $K$  increased. It is indicated in figures 10 and 11 that, as would be expected, this trend carries over to the case of lifting bodies.

It appears in figures 10 and 11 that the most important factor influencing the accuracy of the method is the reliability of the conical flow theory at the vertex, since the inaccuracies at the vertex appear to be reflected strongly in the pressures downstream of the vertex. The question naturally arises, then, how good are the predictions of the shock-expansion method when experimentally determined initial conditions at the vertex are employed? To answer this question, the pressure coefficients on the surfaces of the two ogives under discussion were determined in the following manner. Initial conditions at the vertex were determined from the measured static pressures around a cone (corresponding to the vertex angle of the body) in conjunction with the measured shock-wave angle (in the plane  $\phi = 0$ ) obtained from schlieren photographs of the conical flow field. The pressure coefficients downstream of the vertex were then calculated as before. The results of these calculations for Mach numbers 3.00, 4.25, and 5.05 are compared with experiment in figures 12 and 13 for  $\alpha = 15^\circ$ . Results for  $\alpha = 15^\circ$  are presented because at this angle of attack the applicability of the conical flow solutions is most marginal. It is observed from figure 12(a) that the theory yields results which indicate an underexpansion of the flow on the sides of the body ( $\phi = 45^\circ$  and  $\phi = 90^\circ$ ). This result is not surprising since, at this low value of  $K$  ( $K = 0.60$ ), it would be expected that the true streamlines would deviate considerably from a meridian line. In other words, flow disturbances in planes tangent to the body at the surface are no longer small compared to those in axial planes. Hence, the flow along a true streamline travels through a greater resultant angle than that represented by a meridian line. It can be seen from figures 12(b) and 12(c) that as the Mach number and, hence,  $K$ , is increased, better agreement is obtained.

---

<sup>8</sup>It should be noted in figure 10(a) that Stone's second-order solution is employed at the vertex since the conical flow theory of the present paper is not applicable for these conditions (i.e.,  $M_0 = 3.00$  and  $\delta_c = 11.42^\circ$ ; see fig. 2).

This is attributed to the fact that the streamlines of the flow deviate less from meridian lines as  $K$  is increased. The same general trend may be noted in figure 13 for the fineness-ratio-3 ogive. However, in this latter case, over-all agreement appears to be better. In fact, good results are obtained for values of  $K > 1$  except on the extreme leeward side of the body where it is probable that viscous effects are influencing the pressures. There may be some separation of flow over this portion of the body although no evidence of this could be determined from the schlieren photographs. In the case of the fineness-ratio-5 ogive, schlieren evidence indicated flow separation on the leeward side of the body for all Mach numbers at  $\alpha = 15^\circ$ . It may be deduced from these figures that the application of the shock-expansion method will yield better results when the initial conditions at the vertex are determined from cone tests rather than from presently available cone theory.

There now remains the determination of the accuracy of the predictions of the generalized shock-expansion method for the flow field (other than the surface) about a lifting body of revolution. To this end, flow in the plane of symmetry ( $\phi = 0^\circ$  and  $\phi = 180^\circ$ ) was calculated (after the manner discussed in Appendix B) for each ogive traveling at a Mach number 5.05 and at an angle of attack of  $10^\circ$ . Flow in a side meridian plane ( $\phi = 90^\circ$ ) was also calculated for the fineness-ratio-3 ogive. The resulting shock-wave shapes are compared with the actual shapes (obtained from schlieren photographs) in figure 14. The theoretically determined conical shocks are also shown for contrast. In the case of the fineness-ratio-3 ogive ( $K = 1.68$  and  $\alpha/\delta_N = 0.53$ ), theory and experiment are observed to be in excellent agreement in the plane of symmetry. The same observations may be made for the side meridian plane. In this latter connection, it is of interest to point out that essentially the same result would have been obtained if the shock were assumed circular in cross-sectional planes and its location determined from the calculations in the plane of symmetry. In view of the agreement between theory and experiment, it is indicated that when  $K$  is greater than 1 and  $\alpha/\delta_N$  is about  $1/2$  or less, the shock is essentially circular in cross-sectional view of the flow field about a pointed body of revolution. In the case of the fineness-ratio-5 ogive, the poor agreement on the leeward side of the body might be expected since not only is  $K$  marginal for the application of the theory but, more important,  $\alpha/\delta_N$  is relatively large ( $\alpha/\delta_N = 0.88$ ). It should be pointed out that if experimentally determined initial conditions are employed, good agreement with experiment downstream of the vertex is obtained.

Although the predictions of the generalized shock-expansion method have been checked only at the inner and outer boundaries of the flow field, it is expected that equally good results would be obtained at intermediate points in the flow field. This conclusion is based on the fact that the bow shock waves were obtained as a result of the calculations of these intermediate points.

### Hypersonic Slender-Body Theory

The predictions of the hypersonic slender-body theory for  $\alpha = 0^\circ$  and  $\alpha = 5^\circ$  are compared with experiment in figures 15 and 16. It appears from a comparison of figures 9 and 15 that the slender-body theory will yield more accurate drag coefficients than the more general theory at  $\alpha = 0^\circ$ , particularly at the lower values of  $K$ . This result, although doubtlessly fortuitous, is the same as that found in reference 1. In the case of lifting bodies, it appears that the slender-body theory yields results which are somewhat less satisfactory at all values of  $K$ . However, the theory displays sufficient accuracy for many engineering purposes even at  $K = 1$ . This is particularly evident for the more slender of the two bodies as indicated in figure 16(b). In view of its simplicity, the slender-body method should prove useful and its application is further facilitated by the presentation in this paper of tabulated values of the pertinent flow parameters for selected values of  $M_0 \delta_N$  and  $\alpha/\delta_N$  (see table I).

### Normal-Force Coefficients

It is appropriate now to consider briefly the forces experienced by the ogives. To this end, normal-force coefficients were obtained by integrating the theoretical pressure distributions for the two ogives at a Mach number of 5.05. The results of these calculations are compared with those obtained from integrated experimental pressure distributions in figure 17 for values of  $K$  of 1.01 and 1.68. It is observed that theory yields values of  $C_N$  which are, in general, higher than those obtained by experiment. However, agreement improves with increasing  $K$ . Equation (36), as well as the hypersonic slender-body solution (eq. (39)), appears to yield satisfactory initial normal-force-curve slopes at values of  $K$  as low as 1. Axial forces have also been obtained for these ogives and the shock-expansion method is found to apply with essentially the same accuracy.

### CONCLUDING REMARKS

The flow about a lifting body of revolution at high supersonic airspeeds was investigated analytically. With the assumptions of conical flow at the vertex, high supersonic Mach numbers, and low angles of attack, simple approximate solutions were obtained which yield the Mach number and pressure distributions on the surface of the body. Surface streamlines were approximated by meridian lines and the flow field in meridian planes was calculated by means of the generalized shock-expansion method. In the special case of slender bodies, simple explicit expressions were obtained for the Mach number and pressure distributions on the surface.

Surface pressures and shock-wave shapes were obtained experimentally at Mach numbers from 3.00 to 5.05 for two ogives having fineness ratios 3 and 5 and for two cones having the same vertex angles as the ogives. The predictions of the methods of this paper for the surface pressures were found to be in good agreement with experiment at values of  $K$  about 1, or greater, when  $\alpha/\delta_N$  (the ratio of angle of attack to semivertex angle) was less than about  $1/2$ . For increasing values of this parameter, agreement deteriorates but may still be considered fair for values of  $\alpha/\delta_N$  up to about 1. The generalized shock-expansion method yielded very good agreement with experiment for the shape of the bow shock at  $K = 1.68$  and  $\alpha/\delta_N = 0.53$ . It was further indicated that the bow shock remains essentially circular in cross section for angles of attack up to approximately one half the semivertex angle when  $K$  is greater than 1.

Ames Aeronautical Laboratory

National Advisory Committee for Aeronautics

Moffett Field, Calif., Jan. 13, 1955

## APPENDIX A

## DETERMINATION OF FLOW CONDITIONS AT THE VERTEX IN THE PLANE OF SYMMETRY

Due to the symmetry of the flow in the plane of symmetry,

$$\frac{\partial u}{\partial \phi} = 0 \quad \frac{\partial v}{\partial \phi} = 0 \quad w = 0$$

Now from the flow geometry

$$u = V \cos(\omega - \delta)$$

$$v = -V \sin(\omega - \delta)$$

and from equation (1a)

$$v = \frac{\partial u}{\partial \omega}$$

The flow is therefore irrotational and the following relation holds

$$\frac{dV}{V} = -\tan(\omega - \delta) d\delta \quad (A1)$$

Substituting the above expressions in equation (5) results in

$$\frac{\gamma - 1}{2} \left[ \left( \frac{\hat{V}}{\bar{V}} \right)^2 - 1 \right] \left[ \cot(\omega - \delta) \left( 1 + \frac{\partial \delta}{\partial \omega} \right) - \cot \omega + \tan(\omega - \delta) \frac{\partial \delta}{\partial \omega} + \right. \\ \left. \frac{\csc(\omega - \delta)}{V \sin \omega} \frac{\partial w}{\partial \phi} \right] - \tan(\omega - \delta) \frac{\partial \delta}{\partial \omega} = 0 \quad (A2)$$

Equation (A2) is not amenable to algebraic solution. However, since it differs only in the term containing  $\partial w / \partial \phi$  from the equivalent equation defining the axisymmetric flow field, a solution analogous to that employed in reference 1 is suggested. Consistent, then, with the restrictions imposed on the flow field in this analysis, namely,  $(\omega - \delta) \ll 1$  radian, equation (A2) reduces to

$$1 - (\omega - \delta) \cot \omega + \frac{\partial \delta}{\partial \omega} [1 - M^2(\omega - \delta)^2] + \frac{1}{V \sin \omega} \frac{\partial \omega}{\partial \phi} = 0 \quad (A3)$$

where  $M$  and, hence, the magnitude of  $V$  are considered constant (see ref. 1). Now from equation (15)

$$\frac{\partial \omega}{\partial \phi} = \pm V_0 \epsilon \frac{\sin \omega_g}{\sin \omega} (1 - \eta \cot \omega_g) \quad (A4)$$

where  $\partial \omega / \partial \phi$  is positive at  $\phi = 0$  and negative at  $\phi = \pi$ . Hence, near the surface of the cone, equation (A3) reduces to the linear equation

$$\frac{\partial \delta}{\partial \omega} = -(1 + \sigma)$$

or

$$\omega - \delta = (\omega - \delta_c)(2 + \sigma) \quad (A5)$$

where (since  $\eta \ll 1$ )

$$\sigma = \pm \frac{V_0}{V} \epsilon \frac{\sin \omega_g}{\sin^2 \delta_c}$$

Combining this relation with equations (A3) and (A5) results in

$$\frac{\partial \delta}{\partial \omega} = \frac{(\omega - \delta_c)(2 + \sigma) \cot \omega - 1}{1 - M^2(\omega - \delta_c)^2(2 + \sigma)^2} - \frac{\sigma \sin^2 \delta_c}{\sin^2 \omega [1 - M^2(\omega - \delta_c)^2(2 + \sigma)^2]} \quad (A6)$$

which can be integrated to yield (substituting in the boundary conditions)

$$\delta - \delta_c = \sigma \sin^2 \delta_c (\cot \omega - \cot \delta_c) \left( 1 - \frac{1}{2} \sin^2 \delta_c \left\{ \csc^2 \left[ \delta_c - \frac{1}{M(2 + \sigma)} \right] + \csc^2 \left[ \delta_c + \frac{1}{M(2 + \sigma)} \right] \right\} \right) +$$

$$\frac{(2 + \sigma) \tan \delta_c \sec^2 \delta_c}{(2 + \sigma)^2 M^2 \tan^2 \delta_c - 1} \ln[1 + (\omega - \delta_c) \cot \delta_c] +$$

$$\frac{\sin^2 \left[ \delta_c - \frac{1}{M(2 + \sigma)} \right] \left\{ \tan \delta_c + M[1 + \sigma + (2 + \sigma)M \tan \delta_c] \right\} - \sigma \sin^2 \delta_c M[1 - (2 + \sigma)M \tan \delta_c]}{2 \sin^2 \left[ \delta_c - \frac{1}{M(2 + \sigma)} \right] (2 + \sigma) M^2 [1 - (2 + \sigma)M \tan \delta_c]}$$

$$\ln[1 + (2 + \sigma)M(\omega - \delta_c)] +$$

$$\frac{\sin^2 \left[ \delta_c + \frac{1}{M(2 + \sigma)} \right] \left\{ \tan \delta_c + M[(2 + \sigma)M \tan \delta_c - (1 + \sigma)] \right\} + \sigma M \sin^2 \delta_c [1 + (2 + \sigma)M \tan \delta_c]}{2 \sin^2 \left[ \delta_c + \frac{1}{M(2 + \sigma)} \right] (2 + \sigma) M^2 [1 + (2 + \sigma)M \tan \delta_c]}$$

$$\ln[1 - (2 + \sigma)M(\omega - \delta_c)] \tag{A7}$$

If  $M$  in equation (A7) is taken as the Mach number just downstream of the shock, then flow conditions at the shock (i.e.,  $M_s$ ,  $\omega_s$ , and  $\delta_s$ ) can be obtained by the simultaneous solution of equations (6), (7), (A7), and the oblique shock-wave relations

$$M_s^2 = \frac{(\gamma + 1)^2 M_o^4 \sin^2(\omega_s \pm \alpha) - 4[M_o^2 \sin^2(\omega_s \pm \alpha) - 1][\gamma M_o^2 \sin^2(\omega_s \pm \alpha) + 1]}{[2\gamma M_o^2 \sin^2(\omega_s \pm \alpha) - (\gamma - 1)][(\gamma - 1)M_o^2 \sin^2(\omega_s \pm \alpha) + 2]} \quad (A8)$$

and

$$\delta_s \pm \alpha = \tan^{-1} \left\{ \frac{\cot(\omega_s \pm \alpha)[M_o^2 \sin^2(\omega_s \pm \alpha) - 1]}{\frac{\gamma + 1}{2} M_o^2 - [M_o^2 \sin^2(\omega_s \pm \alpha) - 1]} \right\} \quad (A9)$$

To apply these equations, a value for  $\epsilon$  is chosen slightly less than  $\alpha$ . Then  $\eta$  is fixed by equation (6) and the relationship between the shock-wave angles is obtained by setting  $\phi = \pi$  in equation (7), namely,

$$(\omega_s)_{\phi=\pi} - (\omega_s)_{\phi=0} = 2\eta \quad (A10)$$

Now  $(\omega_s)_{\phi=0}$  is determined by solving equations (A7), (A8), and (A9) simultaneously where  $\sigma > 0$  in equation (A7) and the positive sign is used in equations (A8) and (A9). Then  $(\omega_s)_{\phi=\pi}$  is determined in the same manner as  $(\omega_s)_{\phi=0}$  where now  $\sigma < 0$  in equation (A7) and the negative sign is used in equations (A8) and (A9). If the resulting value of  $\epsilon$  (calculated from eqs. (6) and (A10)) differs from that originally chosen, the procedure is repeated using the calculated value of  $\epsilon$ , and so forth. Although the foregoing procedure is somewhat tedious, the number of iterations can be reduced to two or three in most cases by carefully choosing  $\epsilon$  and  $(\omega_s)_{\phi=0}$ . In this connection, it has been found useful to choose a value for  $(\omega_s)_{\phi=0}$  which is less than the corresponding shock-wave angle of the nonlifting body by  $\eta$ , the latter angle being approximately 10 to 15 percent of  $\alpha$  at the higher Mach numbers ( $M_o > 4$ ) and 15 to 30 percent of  $\alpha$  at the lower Mach numbers ( $M_o < 4$ ). It should be remembered that  $K$  is always approximately 1.4 or greater in this analysis.

It is clear that equation (A7) should give a better representation of the flow field in the  $\phi = 0$  plane than in the  $\phi = \pi$  plane since  $(\omega - \delta)$  is always less on the high pressure side of the body. In fact, there are cases when the combination of  $M_o$ ,  $\delta_c$ , and  $\alpha$  is such that equation (A7) no longer applies on the leeward side of the body. For example, if the body is slender such that the angle of attack approaches the half-cone angle,  $|\sigma|$  can be 1 or greater. Since  $\sigma < 0$  in this half-plane ( $\phi = \pi$ ),  $\partial\delta/\partial\omega > 0$  for these conditions and equation (A7) will no longer represent  $\delta$  as a monotonically decreasing function of  $\omega$ . Hence, it is possible that no simultaneous solution of equations (A7), (A8), and (A9) will exist in the  $\phi = \pi$  plane. It is necessary, then, to obtain

another expression relating  $\delta$  and  $\omega$  in this plane. The development of such a relationship by imposing the restriction that  $\delta \ll 1$  radian but  $\omega$  remains arbitrary will now be considered.<sup>1</sup>

With the restriction that  $\delta \ll 1$  radian, equation (A2) may be reduced to the form

$$\delta \cot \omega + \frac{\partial \delta}{\partial \omega} [1 - M^2 \sin^2 \omega (1 - \delta \cot \omega)^2] + \frac{1}{V \sin \omega} \frac{\partial w}{\partial \phi} = 0 \quad (A11)$$

where  $M$  is again considered constant. Near the surface of the cone, the above expression reduces to

$$\frac{\partial \delta}{\partial \omega} + \delta \cot \omega + \sigma = 0$$

which has the solution

$$\delta = \sigma \cot \omega + k \csc \omega \quad (A12)$$

Combining equations (A11) and (A12) and integrating the resulting expression yields (to the order of accuracy of this analysis)

$$\frac{\delta}{\delta_c} = \left[ \frac{1 + \frac{2M^2(\sigma+1)(\sin^2 \delta_c - \sin^2 \omega)}{1 + \sqrt{(1 + \sigma M^2 \sin^2 \delta_c)^2 + 4M^2 \sin^2 \delta_c - \sigma M^2 \sin^2 \delta_c}}}{1 + \frac{2M^2(\sigma+1)(\sin^2 \delta_c - \sin^2 \omega)}{1 - \sqrt{(1 + \sigma M^2 \sin^2 \delta_c)^2 + 4M^2 \sin^2 \delta_c - \sigma M^2 \sin^2 \delta_c}}} \right] \frac{1 + \frac{\sigma[(4 + 2\sigma - \sigma^2)M^2 \sin^2 \delta_c - (\sin^2 \delta_c + \sigma)]}{M^2 \sin^2 \delta_c (4 - \sigma^2) - 2\sigma}}{2\sqrt{(1 + \sigma M^2 \sin^2 \delta_c)^2 + 4M^2 \sin^2 \delta_c}} \left( \frac{[2 - \sin^2 \omega (1 + \sigma \csc^2 \delta_c)]^2}{[2 - (\sigma + \sin^2 \delta_c)]^2 \left\{ \frac{\sin^2 \omega}{\sin \delta_c} [1 + (2 + \sigma)M^2 \sin^2 \delta_c - (1 + \sigma)M^2 \sin^2 \omega] - M^2 \sin^2 \delta_c \right\}} \right)^{\frac{\sigma(\sigma + \sin^2 \delta_c)}{2\sigma - M^2 \sin^2 \delta_c (4 - \sigma^2)}} \quad (A13)$$

<sup>1</sup>The method of development is similar to that presented in reference 1.

where  $M$  is again chosen as the Mach number just downstream of the shock. Hence, conditions at the shock can be determined by the iteration procedure mentioned earlier except that now equation (A13) is used in place of equation (A7). Although the former equation may be employed to determine the shock angle at  $\varphi = 0$  as well as at  $\varphi = \pi$  for slender bodies, it is suggested that equation (A7) be used to determine flow conditions on the windward side of the body and equation (A13) for flow conditions on the leeward side of the body only when equation (A7) cannot be solved simultaneously with equations (A8) and (A9). If the shock angles in the plane of symmetry, are known, the variation of  $\delta$  with  $\omega$  is known from equation (A7). For the case where this equation does not apply in the plane  $\varphi = \pi$ , this variation is given by equation (A13).

The determination of the small variations in the local velocity in the plane of symmetry is identical to that presented in reference 1 for the case of  $(\omega - \delta) \ll 1$  radian. Hence, the expression for the velocity may be written

$$\frac{V}{V_S} = \left\{ \frac{\cos(\omega_S - \delta_S)}{\cos \left[ \frac{(\delta_C - \delta)(\omega_S - \delta_S)}{\delta_C - \delta_S} \right]} \right\}^{\frac{\delta_C - \delta_S}{\omega_S - \delta_S}} \quad (A14)$$

If the velocity is known, the Mach number may, of course, be determined from the relation

$$M^2 = \frac{M_S^2 \left( \frac{V}{V_S} \right)^2}{1 - \frac{\gamma - 1}{2} M_S^2 \left[ \left( \frac{V}{V_S} \right)^2 - 1 \right]} \quad (A15)$$

and the pressure coefficient may be obtained with the aid of the expression

$$P = \frac{2}{\gamma M_O^2} \left( \frac{p_S}{p_O} \frac{p}{p_S} - 1 \right) \quad (A16)$$

where

$$\frac{p_S}{p_O} = \frac{2\gamma M_O^2 \sin^2(\omega_S \pm \alpha) - (\gamma - 1)}{\gamma + 1}$$

and

$$\frac{p}{p_S} = \left( \frac{1 + \frac{\gamma - 1}{2} M_S^2}{1 + \frac{\gamma - 1}{2} M^2} \right)^{\frac{\gamma}{\gamma - 1}}$$

## APPENDIX B

## DETERMINATION OF FLOW IN A MERIDIAN PLANE

Flow about a lifting body of revolution may be calculated in any meridian plane by the generalized shock-expansion method in much the same manner as the procedure employed in reference 4 for flow about airfoils. However, the application of the method is somewhat more complicated for the case of a body of revolution since now the influence of the conical flow in the region of the vertex must be considered.

The determination of axially symmetric flow in the region of the vertex of a body of revolution ( $K > 1$ ) was described in reference 16. Expressions were developed which yield the shock-wave curvature as well as flow conditions along a line a short distance downstream of the vertex. An analysis entirely analogous to that in reference 16 was carried through for the lifting body and it was found that more general expressions can be obtained which take into account the effects of angle of attack. Thus, it can be shown that the expression for the ratio of the shock-wave curvature to body curvature near the vertex is (consistent with the assumptions of the present paper)

$$\frac{K_S}{K_N} = \frac{2\gamma M_O^2 \sin^2[\omega_S + \alpha(\cos \varphi + \eta \cot \omega_S \sin^2 \varphi)] - (\gamma - 1)}{M_O^2 \sin^2 \beta_N \sin 2[\omega_S + \alpha(\cos \varphi + \eta \cot \omega_S \sin^2 \varphi)]} [1 - \tan(\omega_S - \delta_N) \cot \beta_N]^{\frac{1}{2\psi}} \quad (B1)$$

where

$$\omega_S = (\omega_S)_{\varphi=0} + \eta(1 - \cos \varphi)$$

The function  $\psi$  is defined by the expression

$$\psi = \left(1 + \frac{1}{V \sin \delta_N} \frac{\partial w}{\partial \varphi}\right) \left[1 - M^2 \left(\frac{w}{V}\right)^2\right]$$

and is evaluated at the surface outside the vortical layer by means of the previously developed conical-flow expressions. Similarly, expressions for flow conditions along a line normal to the axis of the body a short distance downstream of the vertex may be obtained. For example, the variation of flow inclination,  $\delta$ , along this line is given by

$$\delta \approx \delta_A - \frac{\psi \sin \delta_A \cos \delta_A}{y_A} (y - y_A) + \left[ \delta_B - \delta_A + \frac{\psi \sin \delta_A \cos \delta_A}{y_A} (y_B - y_A) \right] \left( \frac{y - y_A}{y_B - y_A} \right)^2 \quad (B2)$$

where A and B are points on the line corresponding to the surface and the shock, respectively. The relations for the static pressure and total pressure remain unchanged and may be written (in the notation of the present paper)

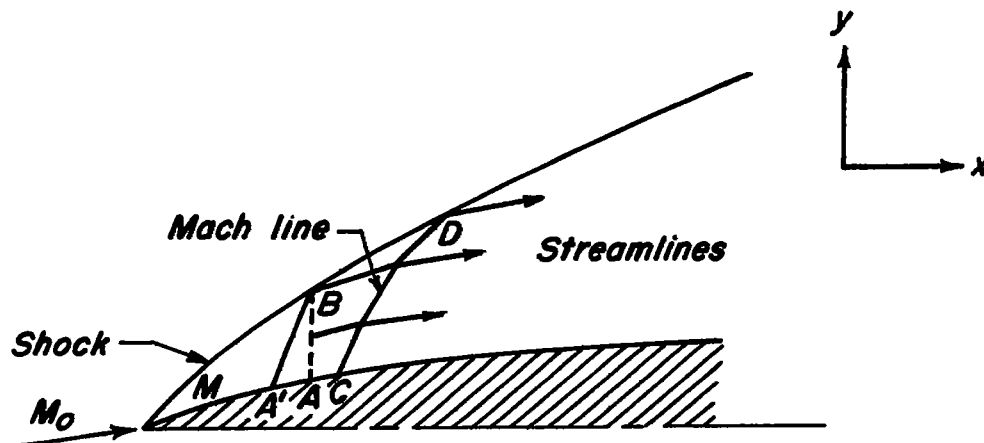
$$p \approx p_A - \left[ \frac{2\gamma p K_N \cos(\beta + \delta)}{\sin \beta \sin 2\beta} \right]_A (y - y_A) + \left\{ p_B - p_A + \left[ \frac{2\gamma p K_N \cos(\beta + \delta)}{\sin \beta \sin 2\beta} \right]_A (y_B - y_A) \right\} \left( \frac{y - y_A}{y_B - y_A} \right)^2 \quad (B3)$$

and

$$H \approx H_B + \left[ \frac{\frac{\partial H}{\partial \omega} K_S \cos \delta}{\sin(\omega - \delta)} \right]_B (y - y_B) + \left\{ H_A - H_B - \left[ \frac{\frac{\partial H}{\partial \omega} K_S \cos \delta}{\sin(\omega - \delta)} \right]_B (y_A - y_B) \right\} \left( \frac{y - y_B}{y_A - y_B} \right)^2 \quad (B4)$$

respectively. It should be noticed that expressions (B1) and (B2) reduce identically to those given in reference 16 for axially symmetric flow.

Knowing the flow conditions in any meridian plane in the region of the vertex, it is now a relatively simple matter to construct the entire flow field downstream of the vertex. To illustrate, consider the sketch (flow in a meridian plane  $\phi = \text{constant}$ ):



With the oblique-shock-wave, conical-flow, and expansion equations, all fluid properties at points M, A', A, C, and so forth, on the body surface may be calculated in the manner described previously in the present paper. Hence, flow conditions along the line AB may be determined from expressions (B1) through (B4). It will be recalled that the basic condition employed in constructing flow fields about airfoils by the generalized shock-expansion method is that the pressure is constant along Mach lines emanating from the surface. In the case of flow about bodies of revolution, this condition must be relaxed to account for the variation in pressure due to the influence of the conical flow in the region of the vertex. This may be accomplished in the following manner. The Mach line A'B is constructed from the known conditions in the region MAB shown in the sketch. The net pressure change along this Mach line (i.e.,  $p_B - p_{A'}$ ) is thus determined. This pressure difference is then assumed to represent the net pressure change between the body surface and the shock along each Mach line emanating from the surface downstream of the vertex. The flow field is then constructed using this criterion in conjunction with the isentropic expansion relations for flow along streamlines. Once the shapes of the streamlines are calculated, the fluid properties along these lines are, of course, determined in the same manner as those along the surface.

## APPENDIX C

FLOW AT THE SURFACE OF A SLENDER BODY TRAVELING AT HIGH  
SUPERSONIC AIRSPEEDS AND AT SMALL ANGLES OF ATTACK

If a slender body (i.e., a body on the surface of which the slopes are everywhere small compared to 1) is traveling at free-stream Mach numbers very large compared to 1 (again, of course,  $K > 1$ ) and at angles of attack very small compared to 1, the local Mach numbers will likewise be large compared to 1. It follows, then, that the inclination of the nose shock wave will be small and, consequently, that  $\omega$  will always be small. In this case, the relation between  $\delta$  and  $\omega$  at the vertex (in the plane  $\phi = 0$ ) is relatively simple and may be obtained by integrating the expression (see eqs. (A4) and (A11))

$$\frac{\partial \delta}{\partial \omega} = -\frac{\delta}{\omega} - \frac{\epsilon \omega_S}{\omega^2}$$

which yields

$$\delta = \frac{\delta_N^2}{\omega} - \frac{\epsilon \omega_S}{\omega} \left( 1 - \frac{\delta_N}{\omega_S} \right) \quad (C1)$$

Combining this expression with equation (A1), the relation

$$\frac{v}{v_S} = \left( \frac{\omega}{\omega_S} \right)^{\delta_N^2} e^{\frac{1}{2}(\delta^2 - \delta_S^2) + \epsilon \delta_N \left( 1 - \frac{\omega_S}{\omega} \right)} \quad (C2)$$

defining the velocities in the plane  $\phi = 0$  is easily obtained. Hence, the surface Mach number in this plane at the vertex,  $M_N$ , may (to the order of accuracy of this analysis) be related to  $M_S$  by combining equation (A15) with equation (C2) to yield

$$M_N^2 = M_S^2 \left\{ 1 + \frac{\gamma - 1}{2} (M_S \delta_N)^2 \left[ 1 + \ln \left( \frac{\delta_N}{\omega_S} \right)^2 - \left( \frac{\delta_S}{\delta_N} \right)^2 - 2 \frac{\epsilon}{\delta_N} \left( \frac{\omega_S}{\delta_N} - 1 \right) \right] \right\} \quad (C3)$$

Now the oblique shock-wave relations for flow of the type under consideration reduce to (at  $\phi = 0$ )

$$M_S^2 = \frac{(\gamma + 1)^2 M_O^4 (\omega_S + \alpha)^2}{[2\gamma M_O^2 (\omega_S + \alpha)^2 - (\gamma - 1)][(\gamma - 1) M_O^2 (\omega_S + \alpha)^2 + 2]} \quad (C4)$$

$$M_O^2 (\omega_S + \alpha)^2 - \frac{\gamma + 1}{2} M_O^2 (\omega_S + \alpha) (\delta_S + \alpha) - 1 = 0 \quad (C5)$$

and

$$\frac{p_S}{p_O} = \frac{2\gamma}{\gamma + 1} M_O^2 (\omega_S + \alpha)^2 - \frac{\gamma - 1}{\gamma + 1} \quad (C6)$$

Combining equations (6), (C1), and (C5) results in

$M_O(\omega_S + \alpha)$

$$= \frac{2}{3} \sqrt{\left(M_O \alpha + \frac{\gamma+1}{2} M_O \eta\right)^2 + 3 \left[1 + \frac{\gamma+1}{2} M_O^2 (\delta_N + \alpha) (\delta_N - \eta)\right]} \\ \cos \left( \frac{1}{3} \cos^{-1} \frac{2\gamma M_O \alpha - 9 \left(M_O \alpha + \frac{\gamma+1}{2} M_O \eta\right) \left[1 + \frac{\gamma+1}{2} M_O^2 (\delta_N + \alpha) (\delta_N - \eta)\right] - 2 \left(M_O \alpha + \frac{\gamma+1}{2} M_O \eta\right)^3}{2 \left\{ \left(M_O \alpha + \frac{\gamma+1}{2} M_O \eta\right)^2 + 3 \left[1 + \frac{\gamma+1}{2} M_O^2 (\delta_N + \alpha) (\delta_N - \eta)\right] \right\}^{\frac{3}{2}}} \right) + \\ \frac{1}{3} \left(M_O \alpha + \frac{\gamma+1}{2} M_O \eta\right) \quad (C7)$$

and

$$\left(\frac{\delta_S}{\delta_N}\right)^2 = \left[\frac{\delta_N}{\omega_S} - \frac{\epsilon}{\omega_S} \left(\frac{\omega_S}{\delta_N} - 1\right)\right]^2 \quad (C8)$$

There remains now the determination of  $\eta$ , which defines the position of the conical shock, in order to determine the shock-wave angle in the plane  $\phi = 0$ . To this end, the assumption of a circular conical shock is again employed, but now it is deemed sufficiently accurate for the purposes of this analysis to assume a linear variation of  $\eta$  with  $\alpha$ ; namely

$$\eta = \left. \frac{d\eta}{d\alpha} \right|_{\alpha=0} \alpha$$

Now from equation (A10) there results

$$\frac{d\eta}{d\alpha} = \frac{1}{2} \left( \left. \frac{d\omega_S}{d\alpha} \right|_{\varphi=\pi} - \left. \frac{d\omega_S}{d\alpha} \right|_{\varphi=0} \right) \quad (C9)$$

Consider for the moment, flow in the plane  $\varphi = \pi$ . The angle of attack  $\alpha$  and, therefore,  $\epsilon$  are both negative in this plane. Hence, equation (C5) may be written

$$M_0^2(\omega_S - \alpha)^2 - \frac{\gamma + 1}{2} M_0^2(\omega_S - \alpha)(\delta_S - \alpha) - 1 = 0$$

and the conical-flow expression (see eq. (C1)) becomes (at  $\omega = \omega_S$ )

$$\delta_S \omega_S = \delta_N^2 + \epsilon(\omega_S - \delta_N)$$

Differentiating these expressions with respect to  $\alpha$  and combining the resulting expressions yields in the limit as  $\alpha \rightarrow 0$

$$2\omega_S \left( \frac{\partial \omega_S}{\partial \alpha} - 1 \right) - \frac{\gamma + 1}{2} \left[ \frac{\partial \epsilon}{\partial \alpha} (\omega_S - \delta_N) - (\omega_S + \delta_S) \right] = 0 \quad (C10)$$

Proceeding in the same manner for flow in the plane  $\varphi = 0$  (see eqs. (C1) and (C5)) there is obtained

$$2\omega_S \left( \frac{\partial \omega_S}{\partial \alpha} + 1 \right) - \frac{\gamma + 1}{2} \left[ - \frac{\partial \epsilon}{\partial \alpha} (\omega_S - \delta_N) + (\omega_S + \delta_S) \right] = 0 \quad (C11)$$

Combining equations (6), (C9), (C10), and (C11) results in

$$\left. \frac{d\eta}{d\alpha} \right|_{\alpha=0} = \frac{1 - \frac{\gamma + 1}{4} \left( \frac{\delta_N + \delta_S}{\omega_S} \right)}{1 + \frac{\gamma + 1}{4} \left( \frac{\omega_S - \delta_N}{\omega_S} \right)}$$

At  $\alpha = 0$  (see ref. 1)

and

$$\left. \begin{aligned} \frac{\delta_S}{\delta_N} &= \frac{M_0 \delta_N}{\sqrt{1 + \frac{\gamma + 1}{2} (M_0 \delta_N)^2}} \\ M_0 \omega_S &= \sqrt{1 + \frac{\gamma + 1}{2} (M_0 \delta_N)^2} \end{aligned} \right\} \quad (C12)$$

Hence,

$$\eta = \frac{1 - \frac{\gamma + 1}{4} \frac{\delta_S}{\delta_N} \left(1 + \frac{\delta_S}{\delta_N}\right)}{1 + \frac{\gamma + 1}{4} \left(1 - \frac{\delta_S}{\delta_N}\right)} \alpha \quad (C13)$$

where  $\delta_S/\delta_N$  is a function of  $M_0 \delta_N$  only and, of course, is given by equations (C12). The shock-wave angle at  $\varphi = 0$  can now be determined for given values of  $M_0 \delta_N$  and  $M_0 \alpha$  by means of equations (C7) and (C13). Hence, the shock angle around the entire conical shock front may easily be determined with the aid of the expression

$$\omega_S = (\omega_S)_{\varphi=0} + \eta(1 - \cos \varphi) \quad (C14)$$

Surface conditions around the body at the vertex may now be determined after the manner described in the more general analysis of flow about cones. For example, consistent with the assumptions basic to the present analysis, equations (17) and (18) reduce to

$$\frac{w_e}{(V_N)_{\varphi=0}} = \frac{\omega_S}{\delta_N} \epsilon \sin \varphi \quad (C15)$$

and

$$\frac{u_e}{(V_N)_{\varphi=0}} = 1 + \epsilon \omega_S (1 - \cos \varphi) \quad (C16)$$

respectively. Hence, the surface velocity external to the vortical layer at the vertex may be written

$$\left[ \frac{v_e}{(v_N)_{\varphi=0}} \right]^2 = 1 + 2\epsilon\omega_s(1 - \cos \varphi) + \left( \frac{\epsilon\omega_s}{\delta_N} \right)^2 \sin^2 \varphi \quad (C17)$$

and the corresponding Mach number,  $M_e$ , may be related to  $(M_N)_{\varphi=0}$  by combining equation (19) with this expression to yield

$$\left[ \frac{(M_N)_{\varphi=0}}{M_e} \right]^2 = 1 - \frac{\gamma - 1}{2} (M_N \epsilon)_{\varphi=0}^2 \left[ 2 \frac{\omega_s}{\epsilon} (1 - \cos \varphi) + \left( \frac{\omega_s}{\delta_N} \right)^2 \sin^2 \varphi \right] \quad (C18)$$

Consistent with the assumptions basic to the present analysis, the Mach number directly on the surface at the vertex (i.e., inside the vortical layer) may be obtained from the relation (see eq. (20))

$$\left( \frac{M_e}{M_N} \right)^2 = e^{\frac{E_c - E_e}{\gamma c_v}} \quad (C19)$$

where

$$\frac{E_c - E_e}{e \gamma c_v}$$

$$= \left[ \frac{2\gamma M_o^2 (\omega_s + \alpha)_{\varphi=0}^2 - (\gamma - 1)}{2\gamma M_o^2 (\omega_s + \alpha \cos \varphi)_{\varphi=0}^2 - (\gamma - 1)} \right]^{\frac{1}{\gamma}} \left\{ \frac{M_o^2 (\omega_s + \alpha \cos \varphi)_{\varphi=0}^2 [(\gamma - 1) M_o^2 (\omega_s + \alpha)_{\varphi=0}^2 + 2]}{M_o^2 (\omega_s + \alpha)_{\varphi=0}^2 [(\gamma - 1) M_o^2 (\omega_s + \alpha \cos \varphi)_{\varphi=0}^2 + 2]} \right\} \quad (C20)$$

Equations (C3), (C18), and (C19) may now be combined to yield

$$M_N^2 = \frac{(M_s)_{\varphi=0}^2 \left\{ 1 + \frac{\gamma - 1}{2} (M_s \delta_N)_{\varphi=0}^2 \left[ 1 + \ln \left( \frac{\delta_N}{\omega_s} \right)^2 - \left( \frac{\delta_s}{\delta_N} \right)^2 - 2 \frac{\epsilon}{\delta_N} \left( \frac{\omega_s}{\delta_N} - 1 \right) \right] \right\}_{\varphi=0}}{\left( e^{\frac{E_c - E_e}{\gamma c_v}} \right) \left\{ 1 - \frac{\gamma - 1}{2} (M_N \epsilon)_{\varphi=0}^2 \left[ 2 \frac{\omega_s}{\epsilon} (1 - \cos \varphi) + \left( \frac{\omega_s}{\delta_N} \right)^2 \sin^2 \varphi \right] \right\}} \quad (C21)$$

The expressions just derived provide the Mach number on the surface at the vertex. If  $M_N$  is known, the Mach number anywhere on the surface of the body may be obtained by means of the expression (see ref. 1)

$$M = \frac{M_N}{1 - \frac{\gamma - 1}{2} (M_N \delta_N) \left( 1 - \frac{\delta}{\delta_N} \right)} \quad (C22)$$

Now the pressure coefficient is given by the expression

$$P = \frac{2}{\gamma M_o^2} \left[ \left( \frac{p_s}{p_o} \right)_{\varphi=0} \frac{p}{(p_s)_{\varphi=0}} - 1 \right] \quad (C23)$$

The pressure rise across the shock is given by equation (C6) and the ratio of the pressure anywhere on the surface to the pressure at the shock at  $\varphi = 0$  can be expressed (to the order of accuracy of this analysis) in the form

$$\frac{p}{(p_s)_{\varphi=0}} = \left[ \frac{(M_s)_{\varphi=0}}{M} \right]^{\frac{2\gamma}{\gamma-1}}$$

This expression may be combined with equation (C22), and equation (C23) can be written

$$P = \frac{2}{\gamma M_o^2} \left\{ \left( \frac{p_s}{p_o} \right)_{\varphi=0} \left[ \frac{(M_s)_{\varphi=0}}{M_N} - \frac{\gamma-1}{2} (M_s \delta_N)_{\varphi=0} \left( 1 - \frac{\delta}{\delta_N} \right) \right]^{\frac{2\gamma}{\gamma-1}} - 1 \right\} \quad (C24)$$

yielding the pressure coefficient at any point on the surface of the body.

The initial normal-force-curve slope for slender bodies of revolution may easily be determined in the following manner. To the order of accuracy of this analysis, equation (36) may be reduced to the form

$$\left. \frac{dC_N}{d\alpha} \right|_{\alpha=0} = 8 \left( \frac{l}{d} \right)^2 \delta_N \left. \frac{dC_N}{d\alpha} \right|_{TCN} \int_0^1 \frac{p}{p_N} \frac{\beta_N}{\beta} \left( \frac{r}{l} \right) d \left( \frac{x}{l} \right) \quad (C25)$$

Consistent with the assumptions basic to the present analysis, the following relations may be obtained; namely,

$$\frac{\beta_N}{\beta} = \frac{M}{M_N}$$

and

$$\frac{p}{p_N} = \left( \frac{M_N}{M} \right)^{\frac{2\gamma}{\gamma-1}}$$

These expressions may be combined with equation (C22) and (C25) to yield

$$\left. \frac{dC_N}{d\alpha} \right|_{\alpha=0} = 8 \left( \frac{l}{d} \right)^2 \delta_N \left. \frac{dC_N}{d\alpha} \right|_{TCN} \int_0^1 \left[ 1 - \frac{\gamma-1}{2} (M_N \delta_N) \left( 1 - \frac{\delta}{\delta_N} \right) \right]^{\frac{\gamma+1}{\gamma-1}} \left( \frac{r}{l} \right) d \left( \frac{x}{l} \right) \quad (C26)$$

There remains now the determination of the initial normal-force-curve slope for a cone tangent to the body at the vertex. This slope may be expressed as

$$\left. \frac{dC_N}{d\alpha} \right|_{TCN} = \frac{2}{\gamma \pi M_O^2 \delta_N} \int_0^\pi \frac{d}{d\alpha} \left( \frac{p_N}{p_O} \right) \cos \varphi \, d\varphi \quad (C27)$$

Now the ratio of the static pressure anywhere on the surface of a lifting cone ( $\alpha \ll 1$ ) to the free-stream static pressure may be expressed in the form

$$\frac{p_N}{p_O} = \left( \frac{1 - V_e^2}{1 - V_O^2} \right)^{\frac{\gamma}{\gamma-1}} \left( \frac{H}{H_O} \right) \quad (C28)$$

where  $V_e$  is the local velocity externally adjacent to the vortical layer and

$$\frac{H}{H_O} = \left[ \frac{(\gamma+1)M_O^2(\omega_S + \alpha \cos \varphi)^2}{(\gamma-1)M_O^2(\omega_S + \alpha \cos \varphi)^2 + 2} \right]^{\frac{\gamma}{\gamma-1}} \left[ \frac{2\gamma M_O^2(\omega_S + \alpha \cos \varphi)^2 - (\gamma-1)}{\gamma+1} \right]^{-\frac{1}{\gamma-1}} \quad (C29)$$

Differentiating equation (C28) with respect to  $\alpha$  and retaining only terms which are functions of  $\varphi$ , we obtain in the limit as  $\alpha \rightarrow 0$

$$\frac{d}{d\alpha} \left( \frac{p_N}{p_O} \right) = \frac{p_N}{p_O} \frac{\gamma}{M_O^2 \omega_S} \frac{d\epsilon}{d\alpha} \cos \varphi \left\{ \left( \frac{M_N}{M_O} \right)^2 - \frac{(M_O \delta_N)^4}{(M_O \omega_S)^2 \left[ 1 + \frac{\gamma-1}{2} (M_O \delta_N)^2 \right] \left[ 1 + \gamma (M_O \delta_N)^2 \right]} \right\} \quad (C30)$$

From equations (6) and (C13) there may be obtained

$$\frac{d\epsilon}{d\alpha} = \frac{\frac{\gamma+1}{4} \left[ 1 + \left( \frac{\delta_S}{\delta_N} \right)^2 \right]}{1 + \frac{\gamma+1}{4} \left( 1 - \frac{\delta_S}{\delta_N} \right)}$$

Combining this expression with equation (C30) and noting that (see ref. 1)

$$\left( \frac{p_N}{p_O} \right)_{\alpha=0} = [1 + \gamma(M_O \delta_N)^2] \left( \frac{M_S}{M_N} \right)^{\frac{2\gamma}{\gamma-1}}$$

equation (C27) may finally be written

$$\left. \frac{dC_N}{d\alpha} \right|_{TCN} = \frac{\left( \frac{M_S}{M_N} \right)^{\frac{2\gamma}{\gamma-1}} \left[ 1 + \frac{\gamma+3}{2} (M_O \delta_N)^2 \right] \left\{ \left[ 1 + \frac{\gamma-1}{2} (M_O \delta_N)^2 \right] \left[ 1 + \gamma (M_O \delta_N)^2 \right] \left( \frac{M_N}{M_O} \right)^2 - \left( \frac{\delta_S}{\delta_N} \right)^2 (M_O \delta_N)^2 \right\}}{(M_O \delta_N)^2 \left[ \frac{\gamma+5}{\gamma+1} \frac{\delta_N}{\delta_S} - 1 \right] \left[ 1 + \frac{\gamma-1}{2} (M_O \delta_N)^2 \right]} \quad (C31)$$

where  $M_N$ ,  $M_S$ , and  $\delta_S$  may be determined from reference 1 or by setting  $\alpha = 0$  in the pertinent expressions previously derived in the present paper.

## REFERENCES

1. Eggers, A. J. Jr., and Savin, Raymond C.: Approximate Method for Calculating the Flow About Nonlifting Bodies of Revolution. NACA TN 2579, 1951.
2. Van Dyke, Milton D.: A Study of Hypersonic Small-Disturbance Theory. NACA TN 3173, 1954.
3. Eggers, A. J., Jr.: On the Calculation of Flow About Objects Traveling at High Supersonic Speeds. NACA TN 2811, 1952.
4. Eggers, A. J. Jr., and Syvertson, Clarence A.: Inviscid Flow About Airfoils at High Supersonic Speeds. NACA TN 2646, 1952.
5. Mass. Inst. of Tech., Dept. of Elect. Engr., Center of Analysis. Tables of Supersonic Flow Around Cones of Large Yaw, by the Staff of the Computing Section, Center of Analysis, under the direction of Zdenek Kopal. Tech. Rep. no. 5, Cambridge, 1949.
6. Mass. Inst. of Tech., Dept. of Elect. Engr., Center of Analysis. Tables of Supersonic Flow Around Yawing Cones, by the Staff of the Computing Section, Center of Analysis, under the direction of Zdenek Kopal. Tech. Rep. no. 3, Cambridge, 1947.
7. Ferri, Antonio: Supersonic Flow Around Circular Cones at Angles of Attack. NACA TN 2236, 1950.
8. Staff of the Ames Aeronautical Laboratory: Equations, Tables, and Charts for Compressible Flow. NACA Rep. 1135, 1954.
9. Hamaker, Frank M., Neice, Stanford E., and Eggers, A. J., Jr.: The Similarity Law for Hypersonic Flow About Slender Three-Dimensional Shapes. NACA TN 2443, 1951.
10. Eggers, A. J., Jr., and Nothwang, George J.: The Ames 10- by 14-Inch Supersonic Wind Tunnel. NACA TN 3095, 1954.
11. Stone, A. H.: On Supersonic Flow Past a Slightly Yawing Cone. II. Jour. Math. and Phys., vol. XXX, no. 4, Jan. 1952, pp. 200-213.
12. Roberts, Richard C., and Riley, James D.: A Guide to the Use of the M.I.T. Cone Tables. NAVORD Rep. 2606, 1953.
13. Ferri, Antonio: Supersonic Flow Around Circular Cones at Angles of Attack. NACA Rep. 1045, 1951.
14. Ehret, Dorris M.: Accuracy of Approximate Methods for Predicting Pressures on Pointed Nonlifting Bodies of Revolution in Supersonic Flow. NACA TN 2764, 1952.

15. Rossow, Vernon J.: Applicability of the Hypersonic Similarity Rule to Pressure Distributions Which Include the Effects of Rotation for Bodies of Revolution at Zero Angle of Attack. NACA TN 2399, 1951.
16. Eggers, A. J., Jr., and Kraus, Samuel: Approximate Calculation of Axisymmetric Flow Near the Vertex of a Body Traveling at High Supersonic Speeds. Jour. Aero. Sci., vol. 20, no. 3, Mar. 1953, pp. 215-217.

TABLE I.- TABLE OF FUNCTIONS FOR HYPERSONIC SLENDER BODY METHOD

| $\frac{P_0}{P_\infty}$<br>$(M_0/b_H)^2$ for $\varphi = 0$ |       |       |       |       |       |       |
|---|-------|-------|-------|-------|-------|-------|
| $\alpha/b_H$<br>$M_0/b_H$                                 | 0     | 0.20  | 0.40  | 0.60  | 0.80  | 1.00  |
| 0.60  | 4.178 | 4.753 | 5.406 | 6.143 | 6.969 | 7.817 |
| .80   | 2.963 | 3.517 | 4.161 | 4.898 | 5.732 | 6.665 |
| 1.00  | 2.400 | 2.952 | 3.599 | 4.343 | 5.188 | 6.131 |
| 1.20  | 2.094 | 2.649 | 3.301 | 4.052 | 4.903 | 5.853 |
| 1.40  | 1.910 | 2.468 | 3.125 | 3.881 | 4.737 | 5.691 |
| 1.60  | 1.791 | 2.352 | 3.013 | 3.773 | 4.632 | 5.589 |
| 1.80  | 1.709 | 2.273 | 2.937 | 3.700 | 4.562 | 5.518 |
| 2.00  | 1.650 | 2.217 | 2.884 | 3.648 | 4.512 | 5.471 |
| 2.50  | 1.560 | 2.132 | 2.802 | 3.569 | 4.436 | 5.398 |
| 3.00  | 1.511 | 2.086 | 2.759 | 3.529 | 4.396 | 5.359 |

| $\frac{(M_0)_{\varphi=0}}{M_H}$ for $\varphi = 30^\circ$ |       |       |       |       |       |       |
|--|-------|-------|-------|-------|-------|-------|
| $\alpha/b_H$   | 0     | 0.20  | 0.40  | 0.60  | 0.80  | 1.00  |
| $M_0/b_H$  |       |       |       |       |       |       |
| 0.60   | 1.021 | 1.021 | 1.020 | 1.019 | 1.017 | 1.014 |
| .80  | 1.021 | 1.019 | 1.017 | 1.014 | 1.012 | 1.009 |
| 1.00   | 1.019 | 1.017 | 1.013 | 1.010 | 1.007 | 1.004 |
| 1.20   | 1.017 | 1.014 | 1.010 | 1.006 | 1.003 | .9996 |
| 1.40   | 1.016 | 1.012 | 1.007 | 1.004 | .9998 | .9964 |
| 1.60   | 1.014 | 1.010 | 1.005 | 1.001 | .9974 | .9939 |
| 1.80   | 1.013 | 1.008 | 1.004 | .9994 | .9955 | .9919 |
| 2.00   | 1.012 | 1.007 | 1.002 | .9981 | .9940 | .9903 |
| 2.50   | 1.011 | 1.005 | 1.000 | .9954 | .9914 | .9875 |
| 3.00   | 1.010 | 1.004 | .9988 | .9940 | .9897 | .9857 |

| $\frac{(M_0)_{\varphi=0}}{M_H}$ for $\varphi = 120^\circ$ |       |       |       |        |        |        |        |
|---|-------|-------|-------|--------|--------|--------|--------|
| $\alpha/b_H$  | 0     | 0.20  | 0.40  | 0.60   | 0.80   | 1.00   |        |
| $M_0/b_H$   | 0.60  | 1.021 | 1.002 | 0.9803 | 0.9556 | 0.9271 | 0.8942 |
| .80   | 1.021 | .9918 | .9600 | .9247  | .8850  | .8396  | .7896  |
| 1.00  | 1.019 | .9812 | .9405 | .8961  | .8466  | .7891  | .7260  |
| 1.20  | 1.017 | .9717 | .9238 | .8720  | .8139  | .7460  | .6720  |
| 1.40  | 1.016 | .9638 | .9102 | .8527  | .7876  | .7109  | .6320  |
| 1.60  | 1.014 | .9574 | .8993 | .8371  | .7666  | .6868  | .6020  |
| 1.80  | 1.013 | .9523 | .8907 | .8247  | .7501  | .6607  | .5720  |
| 2.00  | 1.012 | .9483 | .8839 | .8152  | .7372  | .6436  | .5520  |
| 2.50  | 1.011 | .9412 | .8723 | .7989  | .7164  | .6161  | .5220  |
| 3.00  | 1.010 | .9369 | .8656 | .7903  | .7053  | .6024  | .5020  |

| $M_0/b_H$ for $\varphi = 0$ |        |        |        |        |        |        |
|-----------------------------|--------|--------|--------|--------|--------|--------|
| $\alpha/b_H$<br>$M_0/b_H$   | 0      | 0.20   | 0.40   | 0.60   | 0.80   | 1.00   |
| 0.60                        | 0.5655 | 0.5577 | 0.5432 | 0.5319 | 0.5203 | 0.5095 |
| .80                         | .7274  | .7070  | .6863  | .6654  | .6444  | .6234  |
| 1.00                        | .8740  | .8415  | .8087  | .7761  | .7440  | .7128  |
| 1.20                        | 1.006  | .9586  | .9120  | .8665  | .8229  | .7815  |
| 1.40                        | 1.123  | 1.060  | .9981  | .9398  | .8850  | .8342  |
| 1.60                        | 1.226  | 1.146  | 1.070  | .9990  | .9338  | .8748  |
| 1.80                        | 1.318  | 1.220  | 1.129  | 1.047  | .9727  | .9064  |
| 2.00                        | 1.397  | 1.282  | 1.178  | 1.086  | 1.004  | .9313  |
| 2.50                        | 1.556  | 1.402  | 1.269  | 1.155  | 1.058  | .9739  |
| 3.00                        | 1.670  | 1.483  | 1.328  | 1.199  | 1.091  | .9996  |

| $\frac{(M_0)_{\varphi=0}}{M_H}$ for $\varphi = 60^\circ$ |       |       |       |       |       |        |        |
|--|-------|-------|-------|-------|-------|--------|--------|
| $\alpha/b_H$   | 0     | 0.20  | 0.40  | 0.60  | 0.80  | 1.00   |        |
| $M_0/b_H$  | 0.60  | 1.021 | 1.016 | 1.009 | 1.001 | 0.9924 | 0.9823 |
| .80  | 1.021 | 1.012 | 1.002 | .9906 | .9790 | .9667  |        |
| 1.00   | 1.019 | 1.007 | .9941 | .9807 | .9670 | .9530  |        |
| 1.20   | 1.017 | 1.003 | .9876 | .9725 | .9572 | .9417  |        |
| 1.40   | 1.016 | .9990 | .9823 | .9658 | .9495 | .9328  |        |
| 1.60   | 1.014 | .9959 | .9781 | .9606 | .9433 | .9258  |        |
| 1.80   | 1.013 | .9933 | .9747 | .9565 | .9384 | .9203  |        |
| 2.00   | 1.012 | .9916 | .9720 | .9531 | .9346 | .9159  |        |
| 2.50   | 1.011 | .9882 | .9672 | .9471 | .9277 | .9086  |        |
| 3.00   | 1.010 | .9862 | .9643 | .9435 | .9235 | .9041  |        |

| $\frac{(M_0)_{\varphi=0}}{M_H}$ for $\varphi = 150^\circ$ |       |       |        |        |        |        |        |
|---|-------|-------|--------|--------|--------|--------|--------|
| $\alpha/b_H$  | 0     | 0.20  | 0.40   | 0.60   | 0.80   | 1.00   |        |
| $M_0/b_H$   | 0.60  | 1.021 | 0.9977 | 0.9716 | 0.9436 | 0.9132 | 0.8797 |
| .80   | 1.021 | .9849 | .9467  | .9060  | .8626  | .8150  | .7630  |
| 1.00  | 1.019 | .9720 | .9228  | .8709  | .8158  | .7579  | .6960  |
| 1.20  | 1.017 | .9606 | .9021  | .8408  | .7756  | .7042  | .6320  |
| 1.40  | 1.016 | .9511 | .8852  | .8161  | .7424  | .6618  | .5820  |
| 1.60  | 1.014 | .9434 | .8716  | .7964  | .7156  | .6277  | .5420  |
| 1.80  | 1.013 | .9373 | .8609  | .7808  | .6942  | .5999  | .5120  |
| 2.00  | 1.012 | .9324 | .8525  | .7686  | .6774  | .5782  | .4820  |
| 2.50  | 1.011 | .9241 | .8379  | .7481  | .6502  | .5429  | .4420  |
| 3.00  | 1.010 | .9190 | .8305  | .7381  | .6368  | .5260  | .4220  |

| $\frac{(M_0)_{\varphi=0}}{M_H}$ for $\varphi = 0$ |       |       |       |       |       |       |       |
|---|-------|-------|-------|-------|-------|-------|-------|
| $\alpha/b_H$                                      | 0     | 0.20  | 0.40  | 0.60  | 0.80  | 1.00  |       |
| $M_0/b_H$   | 0.60  | 1.021 | 1.024 | 1.025 | 1.025 | 1.026 | 1.025 |
| .80   | 1.021 | 1.022 | 1.023 | 1.023 | 1.022 | 1.022 |       |
| 1.00  | 1.019 | 1.020 | 1.020 | 1.020 | 1.019 | 1.019 |       |
| 1.20  | 1.017 | 1.018 | 1.018 | 1.018 | 1.017 | 1.017 |       |
| 1.40  | 1.016 | 1.016 | 1.016 | 1.016 | 1.016 | 1.016 |       |
| 1.60  | 1.014 | 1.015 | 1.015 | 1.015 | 1.015 | 1.015 |       |
| 1.80  | 1.013 | 1.014 | 1.014 | 1.014 | 1.014 | 1.014 |       |
| 2.00  | 1.012 | 1.013 | 1.013 | 1.013 | 1.013 | 1.013 |       |
| 2.50  | 1.011 | 1.011 | 1.012 | 1.012 | 1.012 | 1.012 |       |
| 3.00  | 1.010 | 1.010 | 1.011 | 1.012 | 1.012 | 1.012 |       |

| $\frac{(M_0)_{\varphi=0}}{M_H}$ for $\varphi = 90^\circ$ |       |       |       |        |        |        |        |
|--|-------|-------|-------|--------|--------|--------|--------|
| $\alpha/b_H$   | 0     | 0.20  | 0.40  | 0.60   | 0.80   | 1.00   |        |
| $M_0/b_H$  | 0.60  | 1.021 | 1.009 | 0.9941 | 0.9769 | 0.9573 | 0.9347 |
| .80  | 1.021 | 1.001 | .9804 | .9566  | .9302  | .9002  |        |
| 1.00   | 1.019 | .9940 | .9670 | .9377  | .9056  | .8693  |        |
| 1.20   | 1.017 | .9871 | .9555 | .9221  | .8853  | .8437  |        |
| 1.40   | 1.016 | .9812 | .9463 | .9095  | .8693  | .8237  |        |
| 1.60   | 1.014 | .9767 | .9389 | .8995  | .8565  | .8078  |        |
| 1.80   | 1.013 | .9730 | .9330 | .8916  | .8466  | .7959  |        |
| 2.00   | 1.012 | .9700 | .9283 | .8854  | .8389  | .7870  |        |
| 2.50   | 1.011 | .9648 | .9202 | .8745  | .8263  | .7726  |        |
| 3.00   | 1.010 | .9616 | .9152 | .8684  | .8191  | .7652  |        |

| $\frac{(M_0)_{\varphi=0}}{M_H}$ for $\varphi = 180^\circ$ |       |       |        |        |        |        |        |
|---|-------|-------|--------|--------|--------|--------|--------|
| $\alpha/b_H$  | 0     | 0.20  | 0.40   | 0.60   | 0.80   | 1.00   |        |
| $M_0/b_H$   | 0.60  | 1.021 | 0.9960 | 0.9688 | 0.9405 | 0.9107 | 0.8795 |
| .80   | 1.021 | .9817 | .9423  | .9008  | .8584  | .8157  |        |
| 1.00  | 1.019 | .9687 | .9168  | .8636  | .8097  | .7547  |        |
| 1.20  | 1.017 | .9566 | .8947  | .8316  | .7680  | .7042  |        |
| 1.40  | 1.016 | .9465 | .8766  | .8052  | .7332  | .6631  |        |
| 1.60  | 1.014 | .9384 | .8620  | .7840  | .7047  | .6309  |        |
| 1.80  | 1.013 | .9319 | .8505  | .7672  | .6821  | .6064  |        |
| 2.00  | 1.012 | .9267 | .8415  | .7521  | .6640  | .5809  |        |
| 2.50  | 1.011 | .9178 | .8264  | .7321  | .6351  | .5492  |        |
| 3.00  | 1.010 | .9126 | .8183  | .7218  | .6212  | .5344  |        |

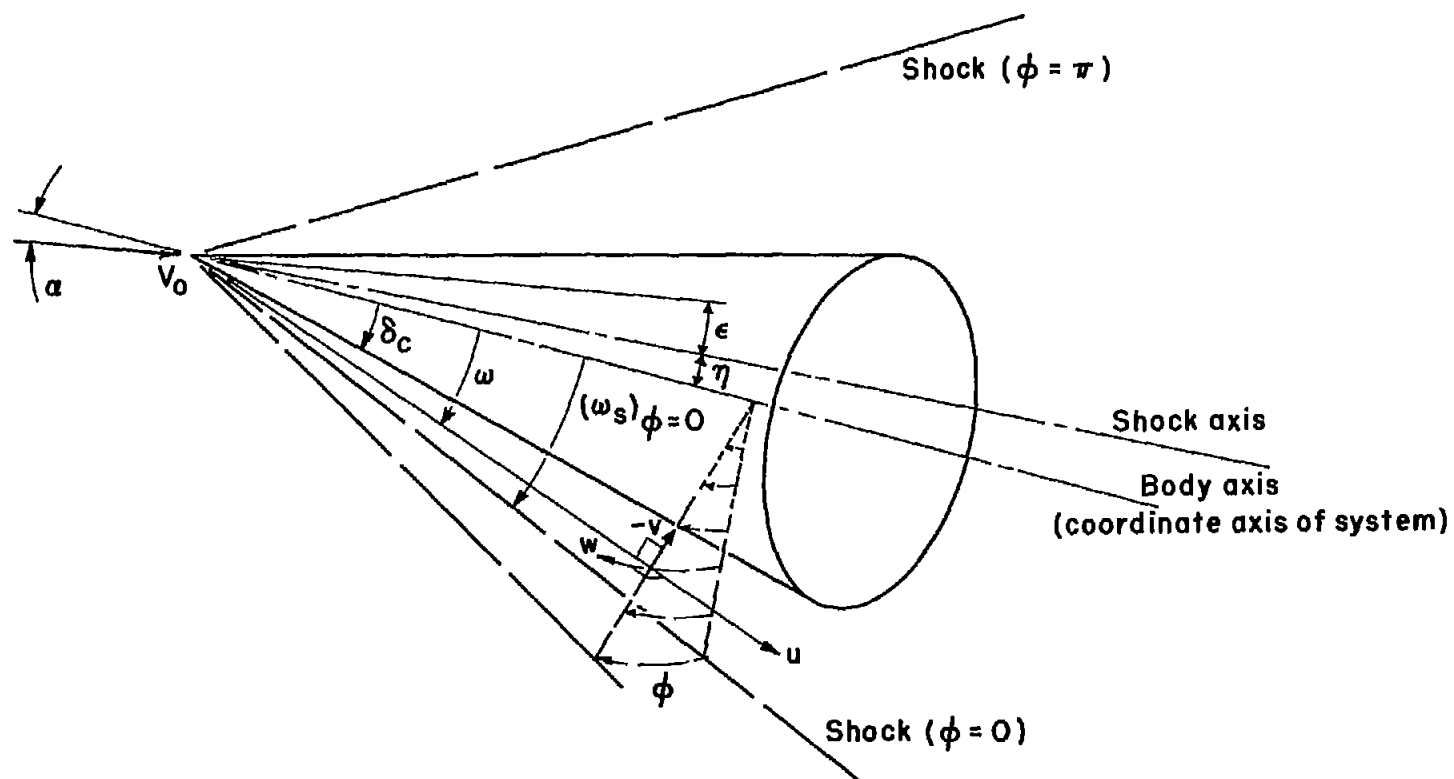


Figure 1.- Schematic diagram of polar coordinate system for determining supersonic flow around a lifting cone.

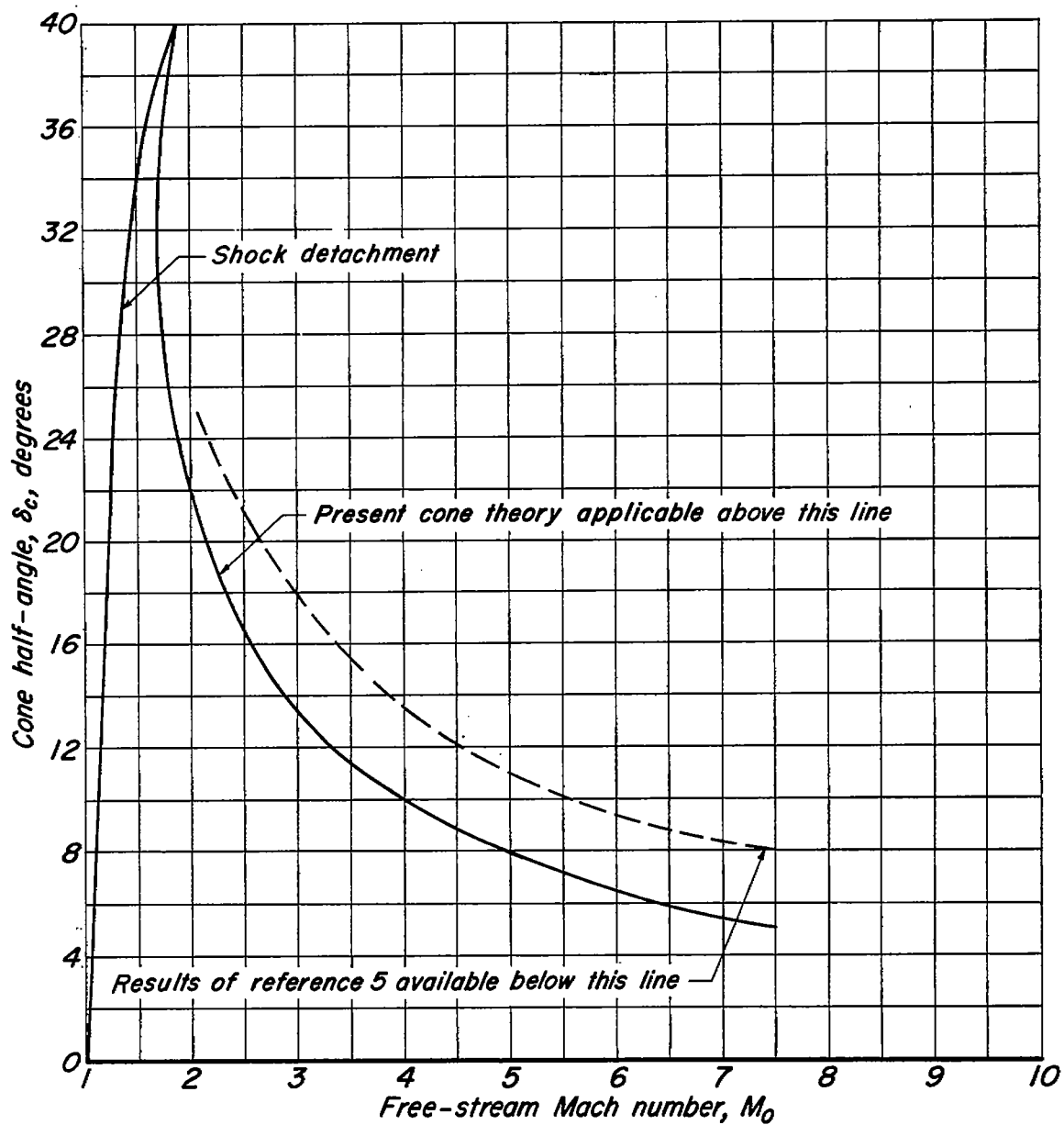
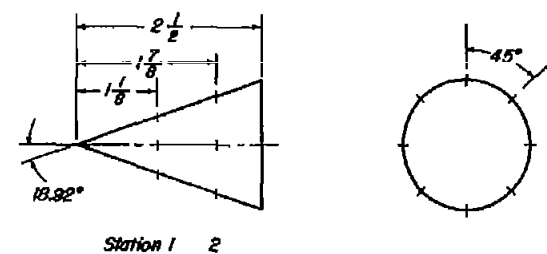
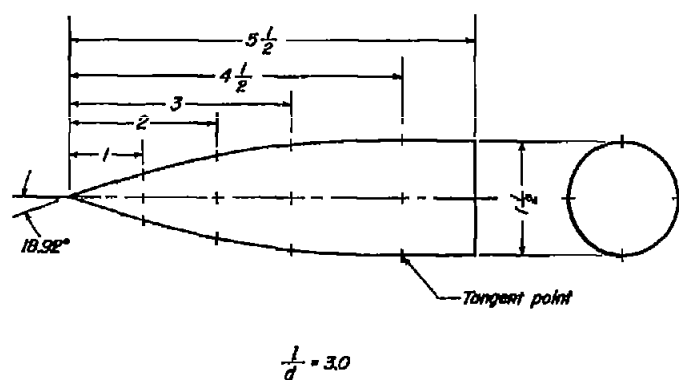
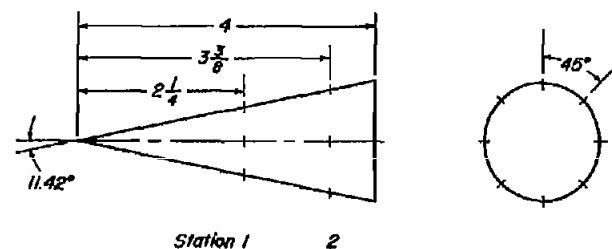
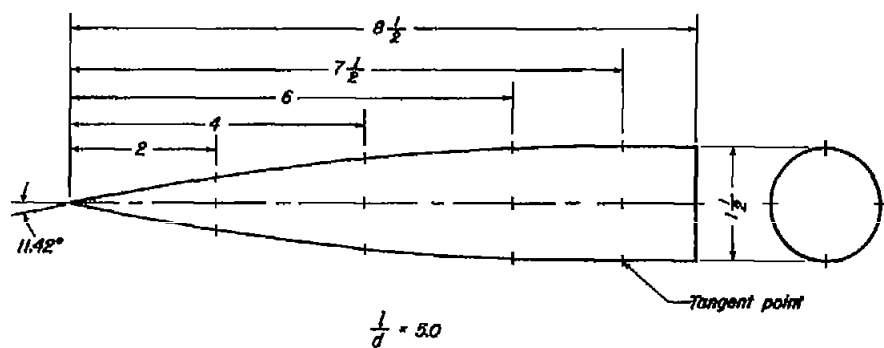


Figure 2.— Variation of cone half-angle with free-stream Mach number showing range of applicability of cone theory.

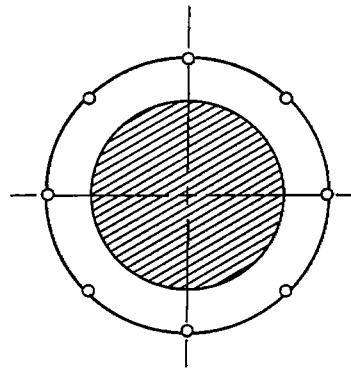
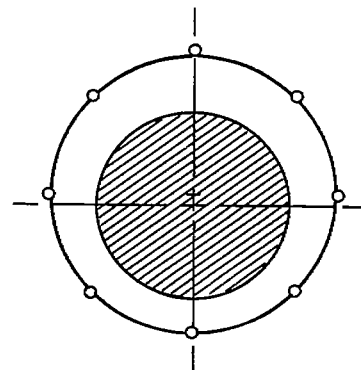


Orifice location shown by +  
All dimensions in inches.

*Circular-arc ogival models*

*Conical models*

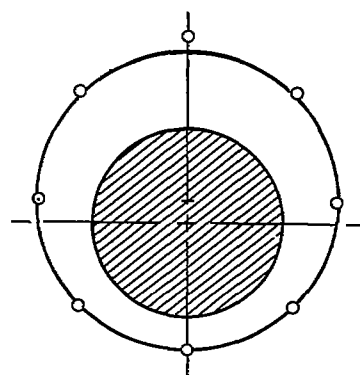
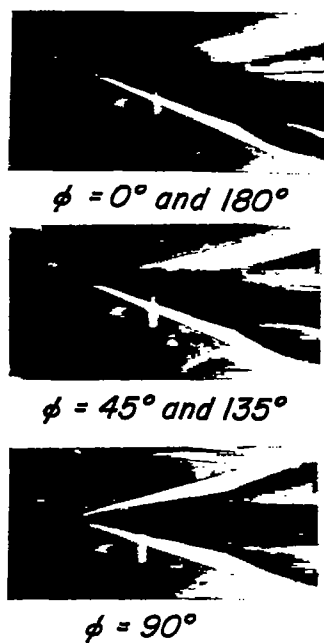
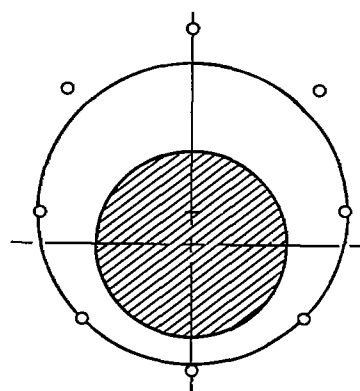
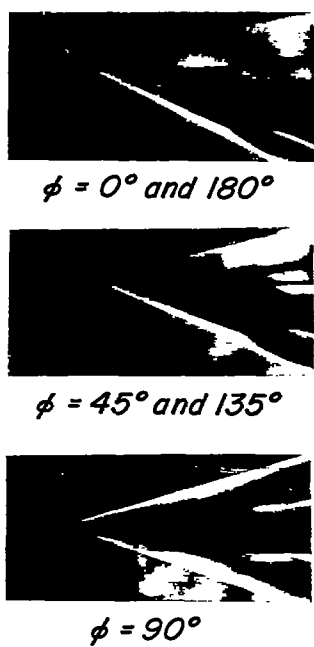
Figure 3.— Dimensions of pressure distribution test models showing location of pressure orifices.

(a)  $\alpha = 0^\circ$  $\phi = 0^\circ$  and  $180^\circ$  $\phi = 45^\circ$  and  $135^\circ$  $\phi = 90^\circ$ 

— Theory

○ Experiment (measured  
from schlieren  
photographs)(b)  $\alpha = 5^\circ$ 

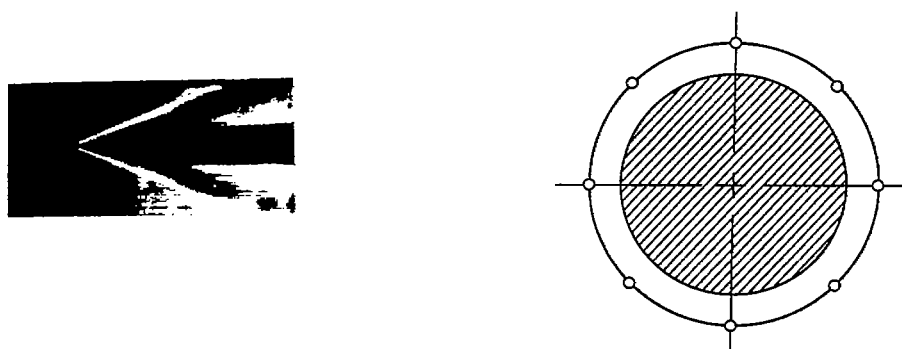
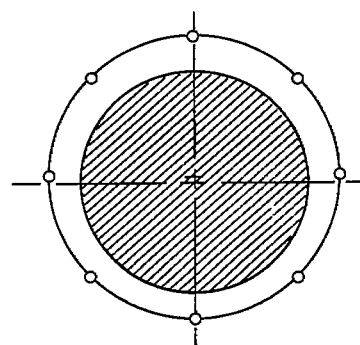
Figure 4.— Shock-wave shapes for an  $11.42^\circ$  semivertex angle cone at  $M_0 = 5.05$  and  $\alpha = 0^\circ, 5^\circ, 10^\circ$ , and  $15^\circ$ .

(c)  $\alpha = 10^\circ$ 

— Theory  
 ○ Experiment (measured from schlieren photographs)

(d)  $\alpha = 15^\circ$ 

Figure 4.— Concluded.

(a)  $\alpha = 0^\circ$  $\phi = 0^\circ$  and  $180^\circ$  $\phi = 45^\circ$  and  $135^\circ$  $\phi = 90^\circ$ 

— Theory

○ Experiment (measured from  
schlieren photographs)(b)  $\alpha = 5^\circ$ 

Figure 5.— Shock-wave shapes for an  $18.92^\circ$  semivertex angle cone at  $M_0 = 5.05$  and  $\alpha = 0^\circ, 5^\circ, 10^\circ$ , and  $15^\circ$ .



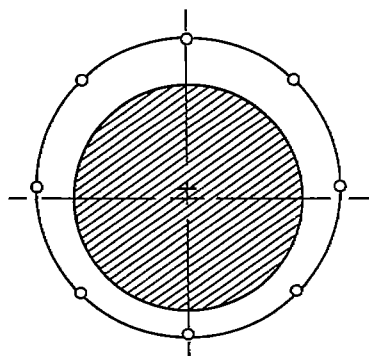
$\phi = 0^\circ \text{ and } 180^\circ$



$\phi = 45^\circ \text{ and } 135^\circ$



$\phi = 90^\circ$



(c)  $\alpha = 10^\circ$



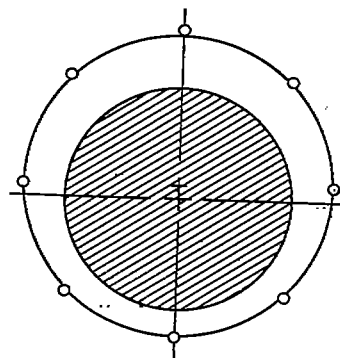
$\phi = 0^\circ \text{ and } 180^\circ$



$\phi = 45^\circ \text{ and } 135^\circ$



$\phi = 90^\circ$



— Theory

○ Experiment (measured from schlieren photographs)

(d)  $\alpha = 15^\circ$

Figure 5.— Concluded.

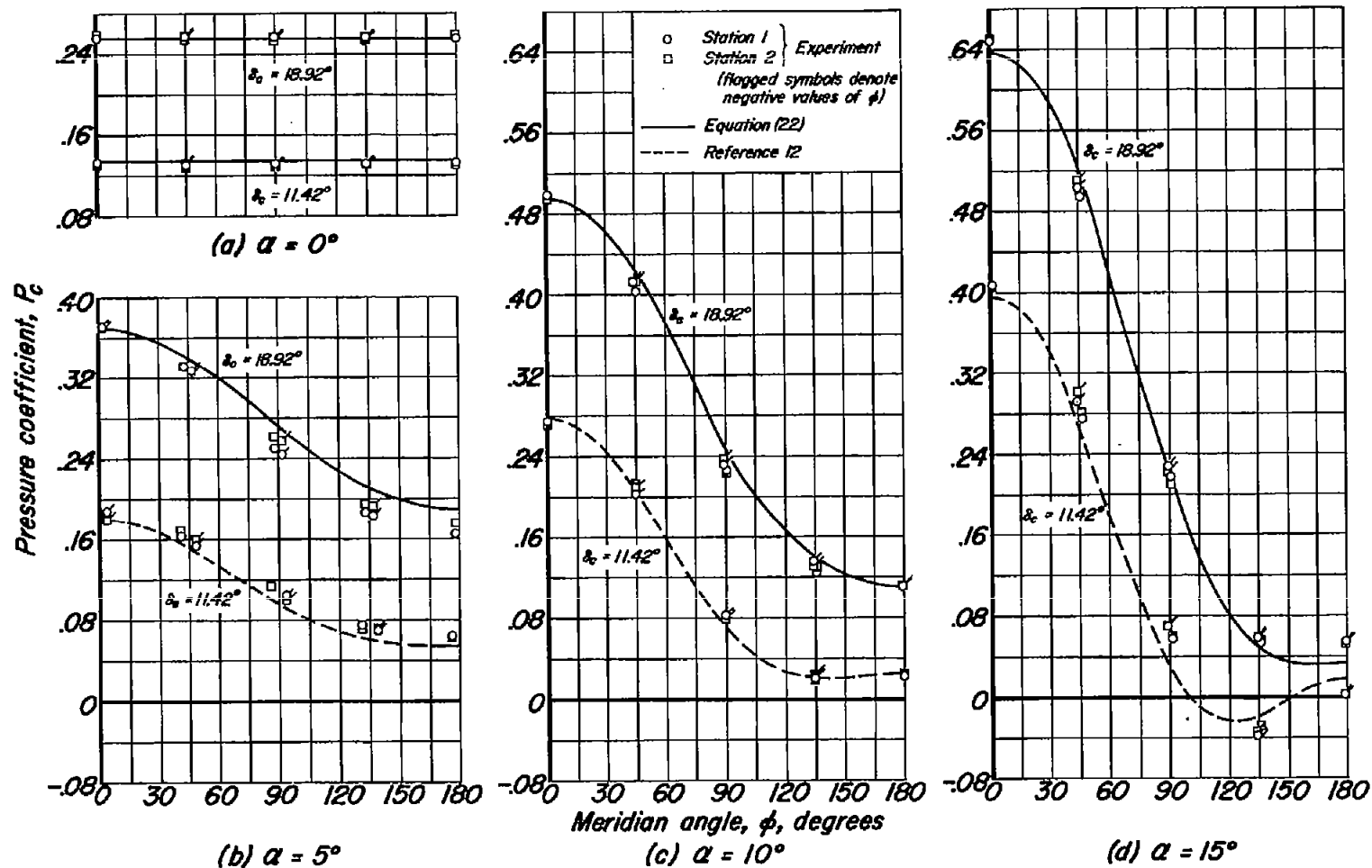


Figure 6.— Circumferential variation of pressure coefficient for two test cones at  $M_0=3.00$  and  $\alpha = 0^\circ, 5^\circ, 10^\circ, \text{ and } 15^\circ$

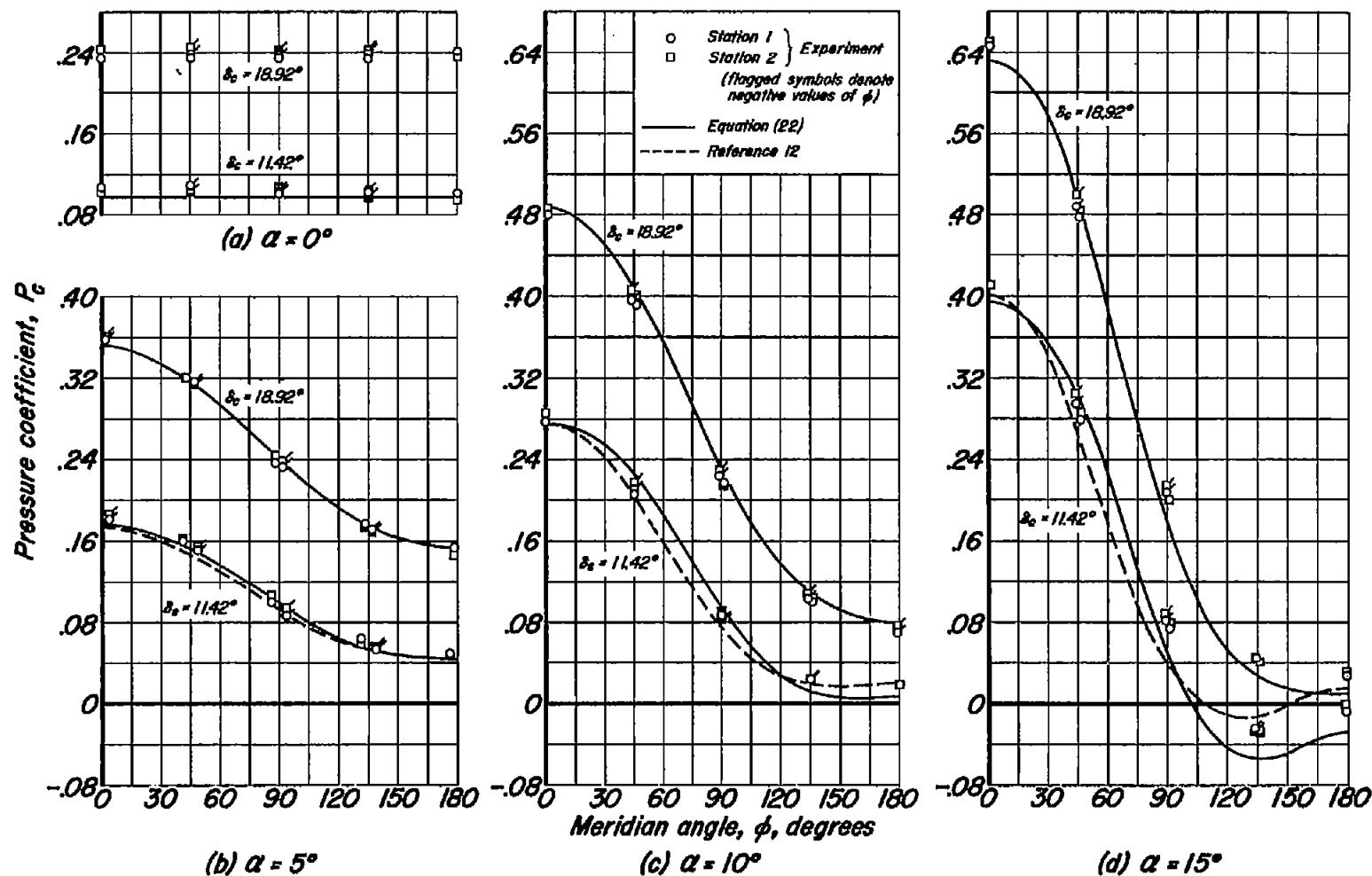


Figure 7.— Circumferential variation of pressure coefficient for two test cones at  $M_0 = 4.25$  and  $\alpha = 0^\circ, 5^\circ, 10^\circ, \text{ and } 15^\circ$ .

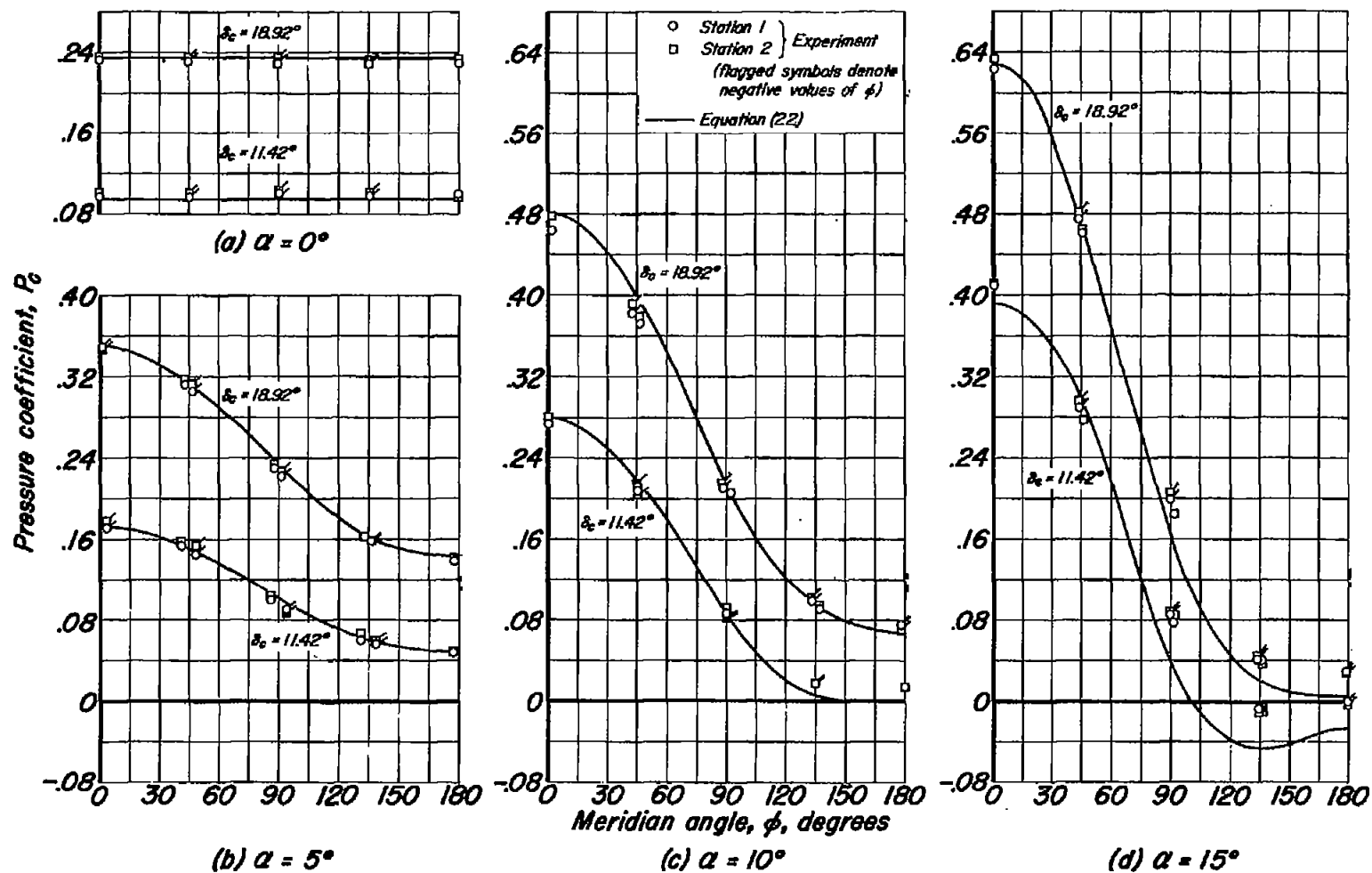


Figure 8.— Circumferential variation of pressure coefficient for two test cones at  $M_0 = 5.05$  and  $\alpha = 0^\circ, 5^\circ, 10^\circ, \text{ and } 15^\circ$

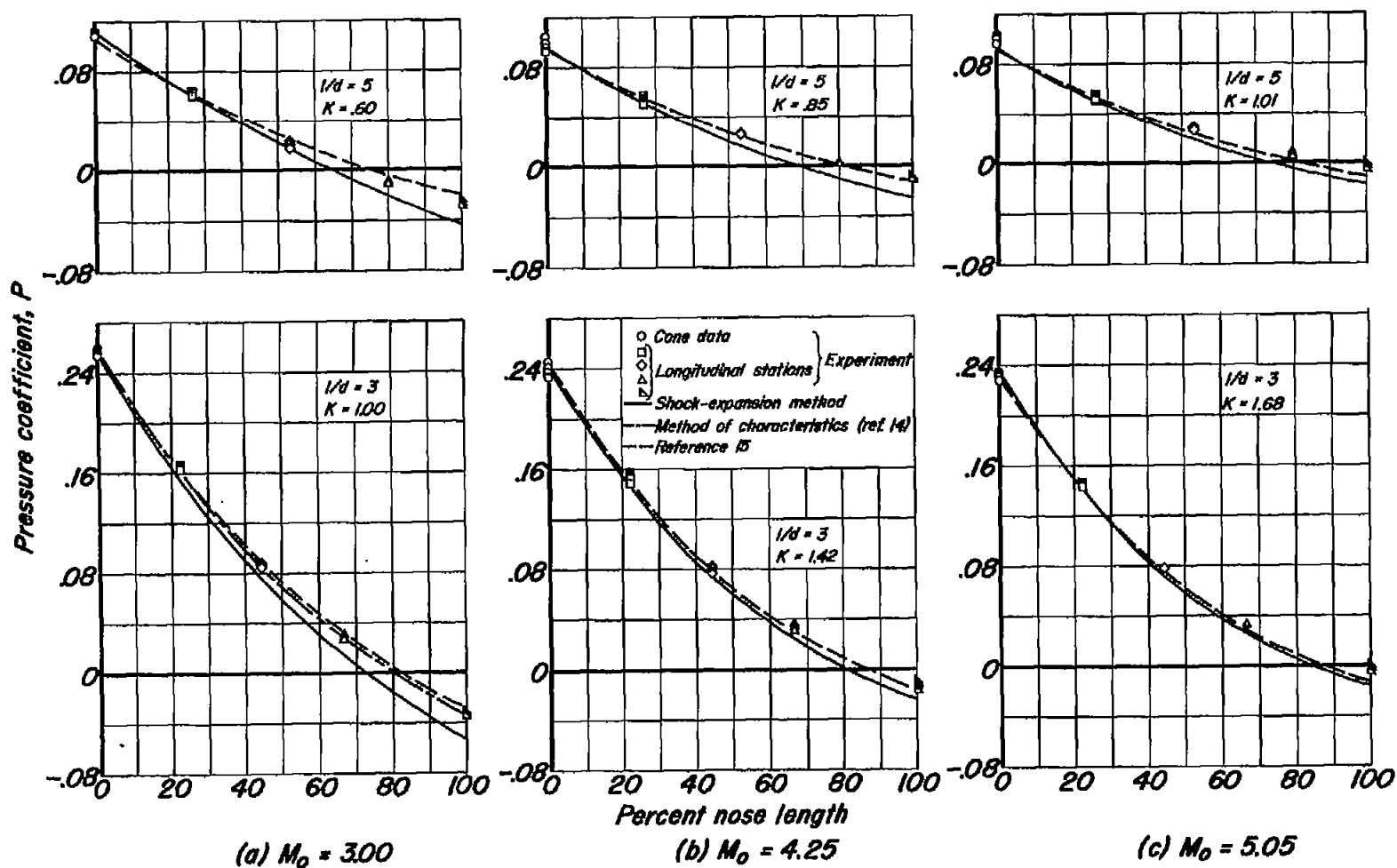
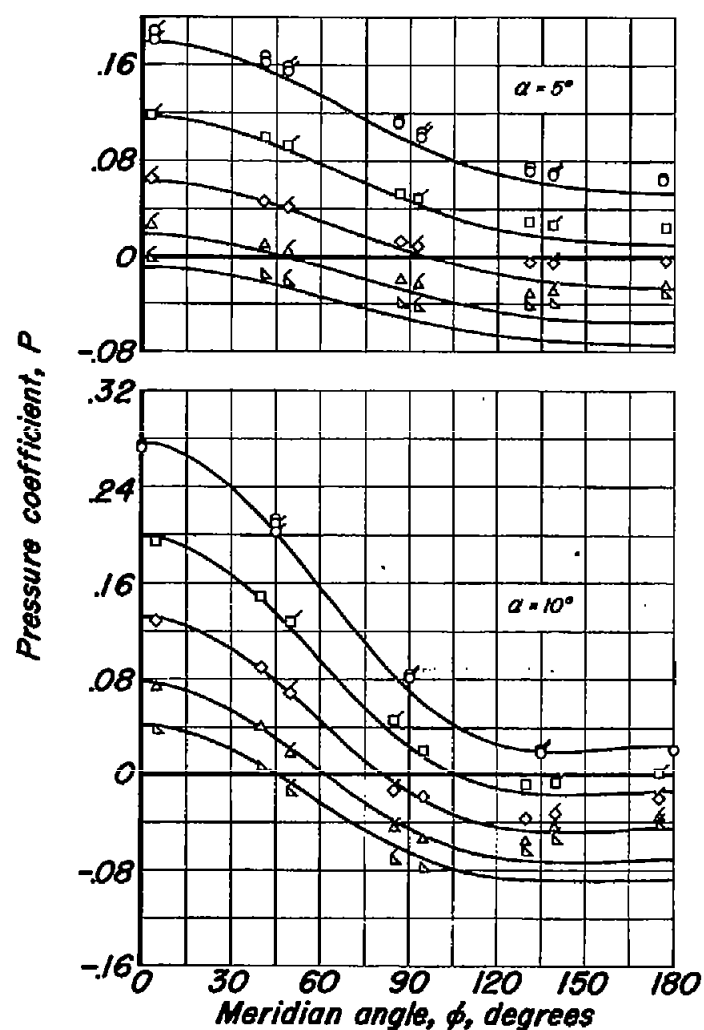
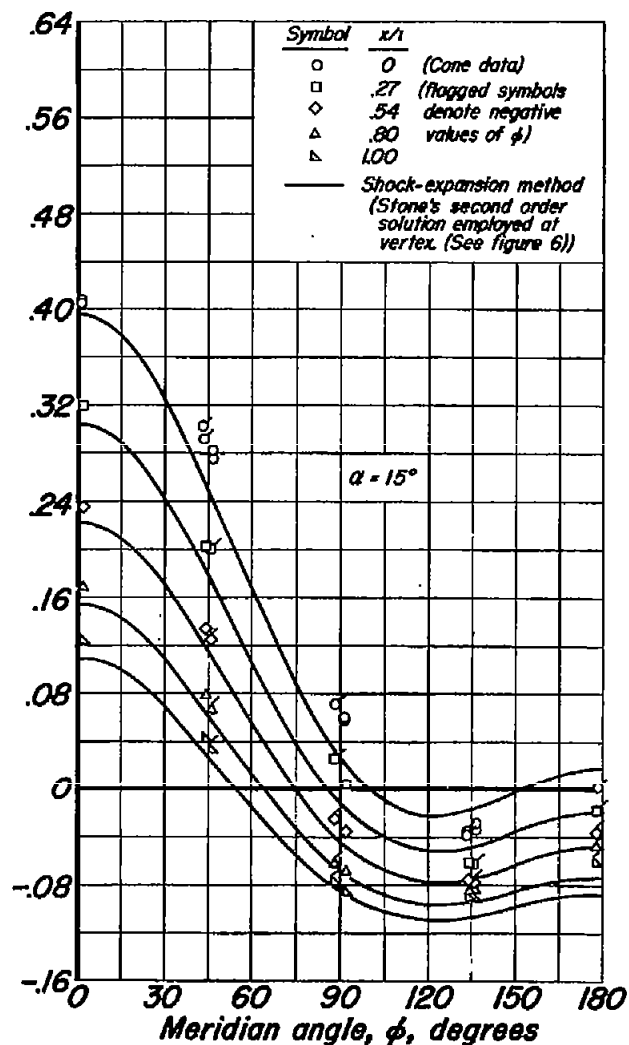


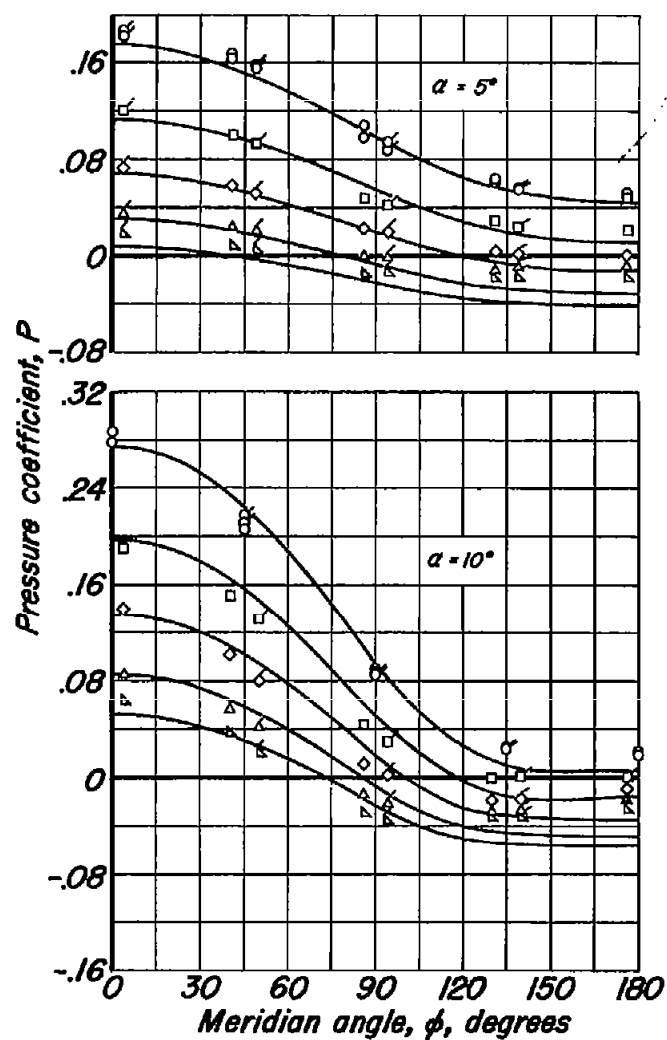
Figure 9.— Variation of pressure coefficient along ogives at  $\alpha = 0^\circ$  and  $M_o = 3.00, 4.25, \text{ and } 5.05$ .



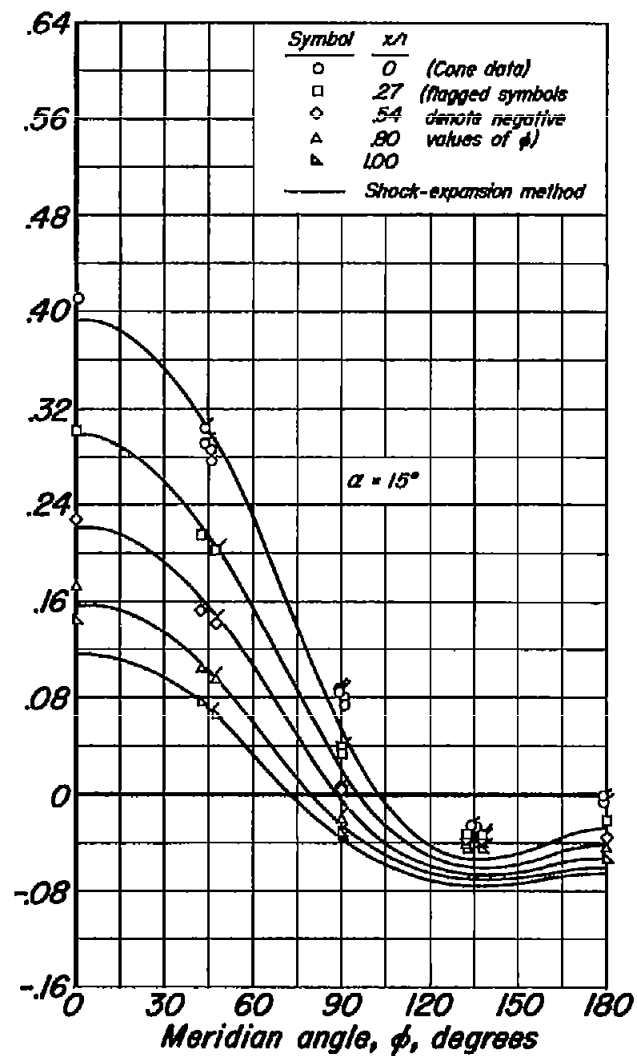
(a)  $M_o = 3.00$ ;  $K = .60$

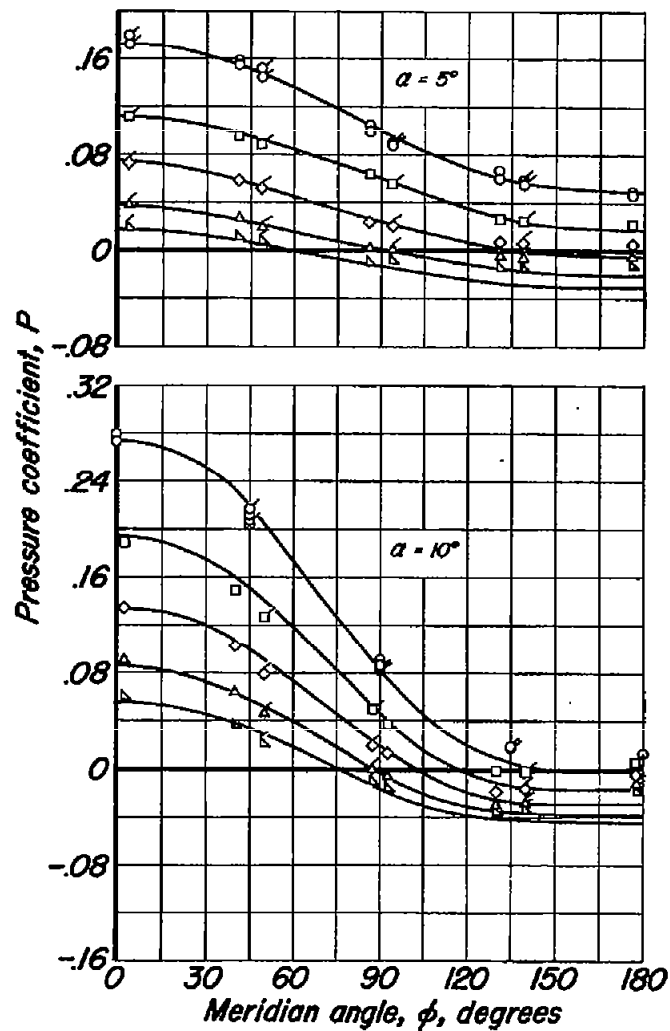
Figure 10.— Circumferential variation of pressure coefficient on a fineness ratio 5 ogive at  $\alpha = 5^\circ$ ,  $10^\circ$ , and  $15^\circ$



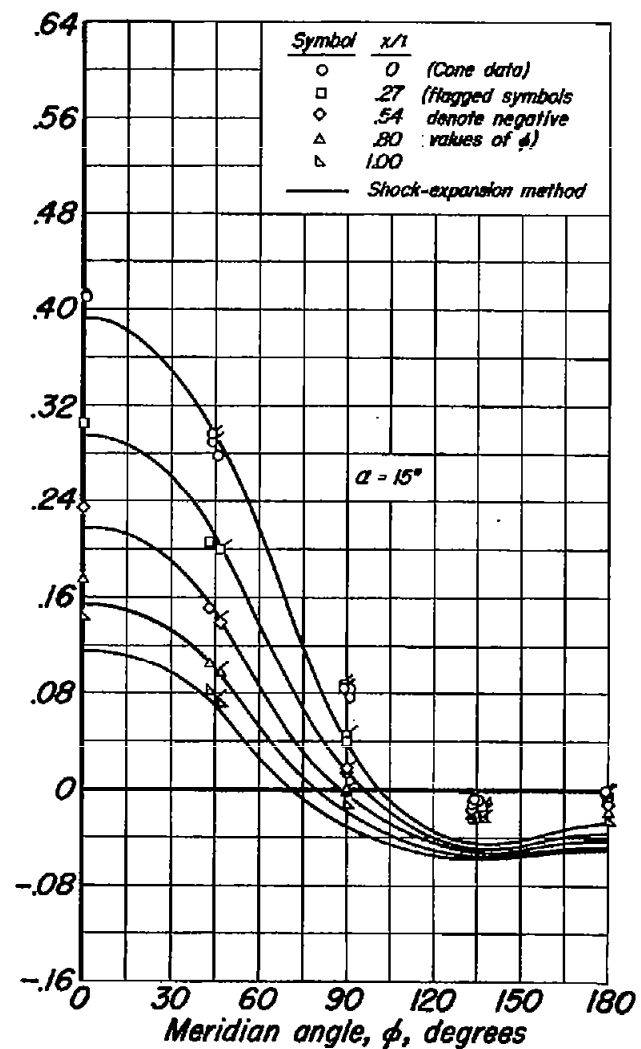


(b)  $M_0 = 4.25$ ,  $K = .85$   
Figure 10.- Continued.





(c)  $M_0 = 5.05$ ;  $K = 1.01$   
Figure 10.- Concluded.



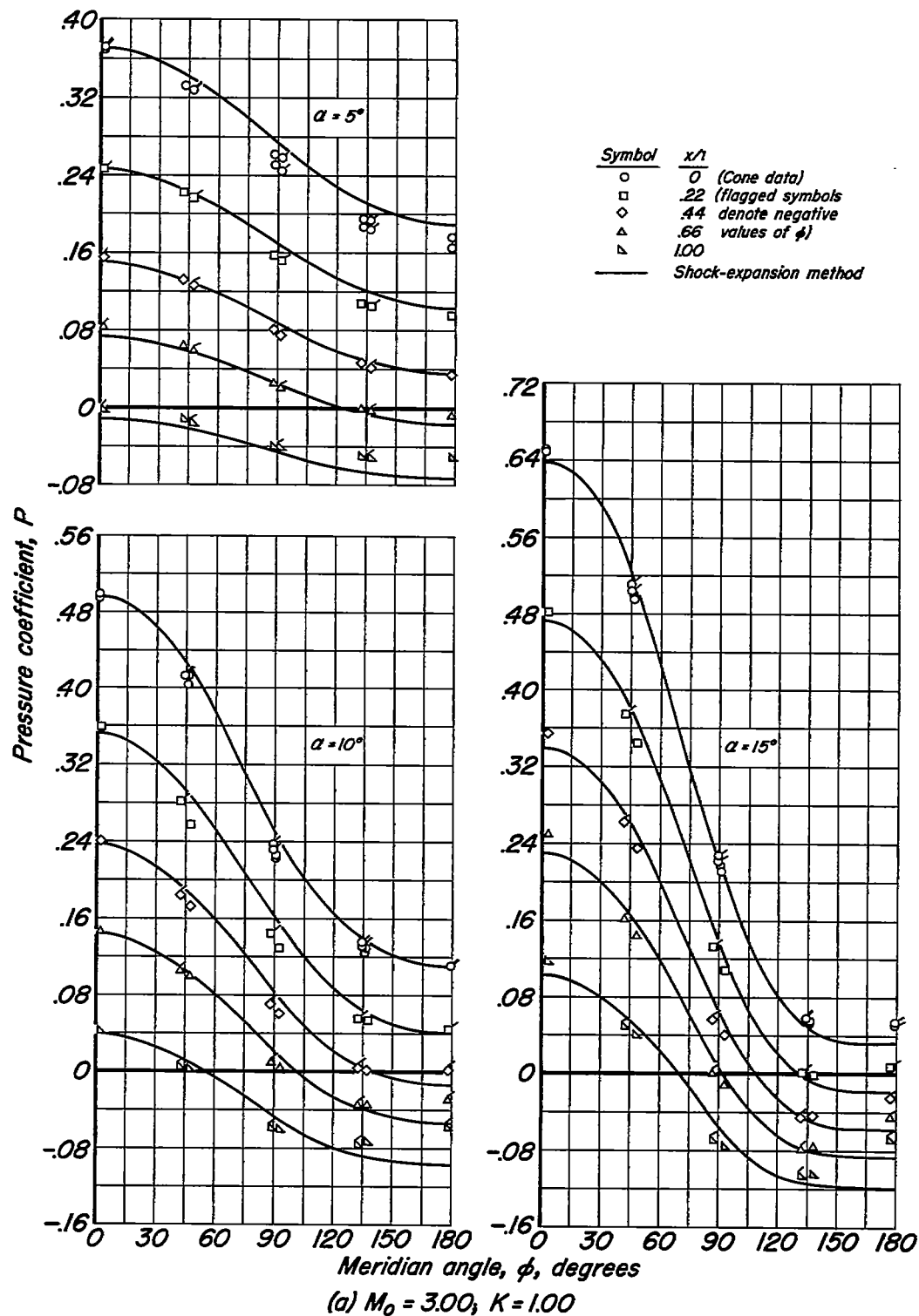


Figure 11.— Circumferential variation of pressure coefficient on a fineness ratio 3 ogive at  $\alpha = 5^\circ, 10^\circ$ , and  $15^\circ$ .

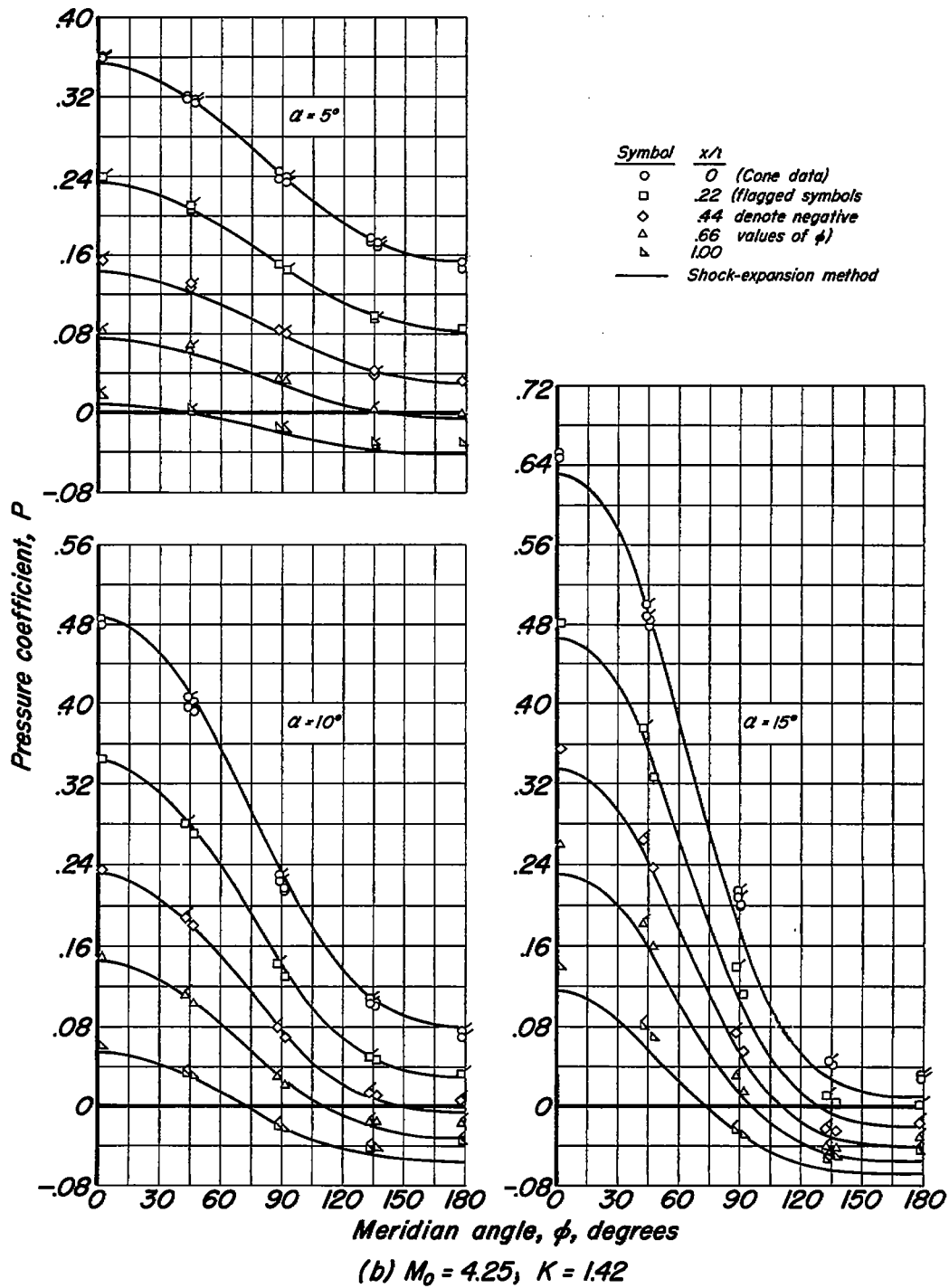


Figure 11.- Continued.

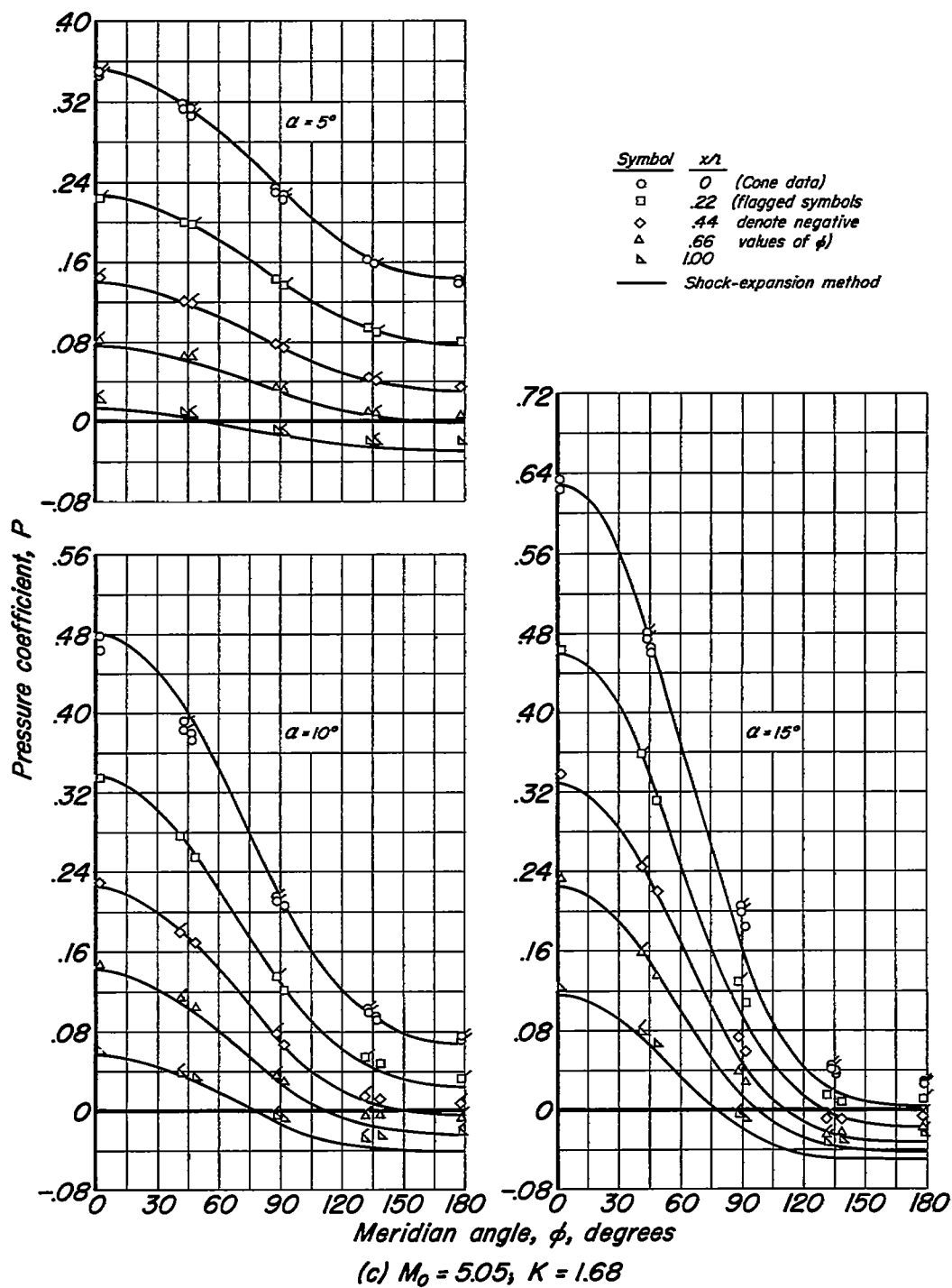


Figure 11- Concluded.

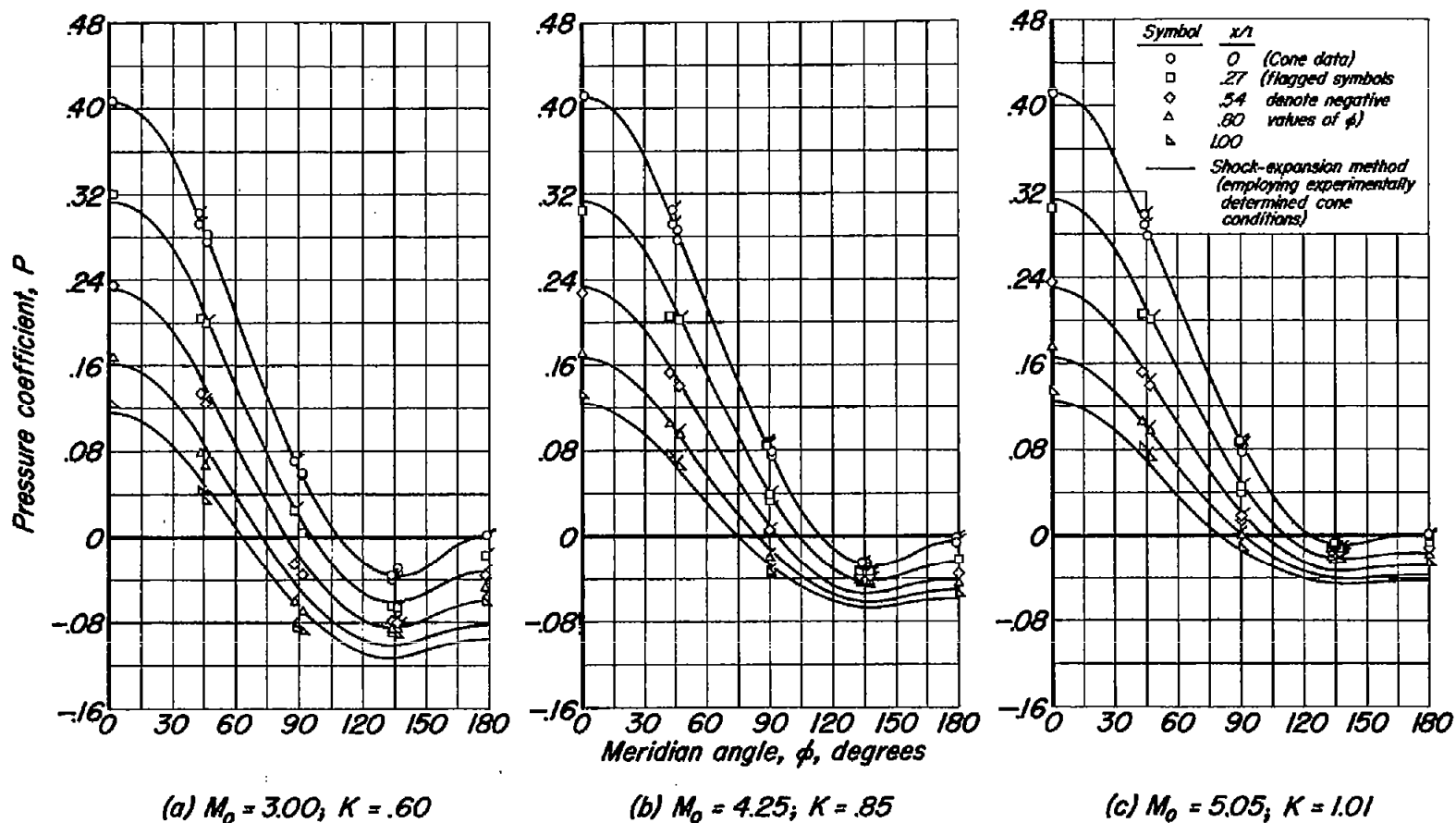
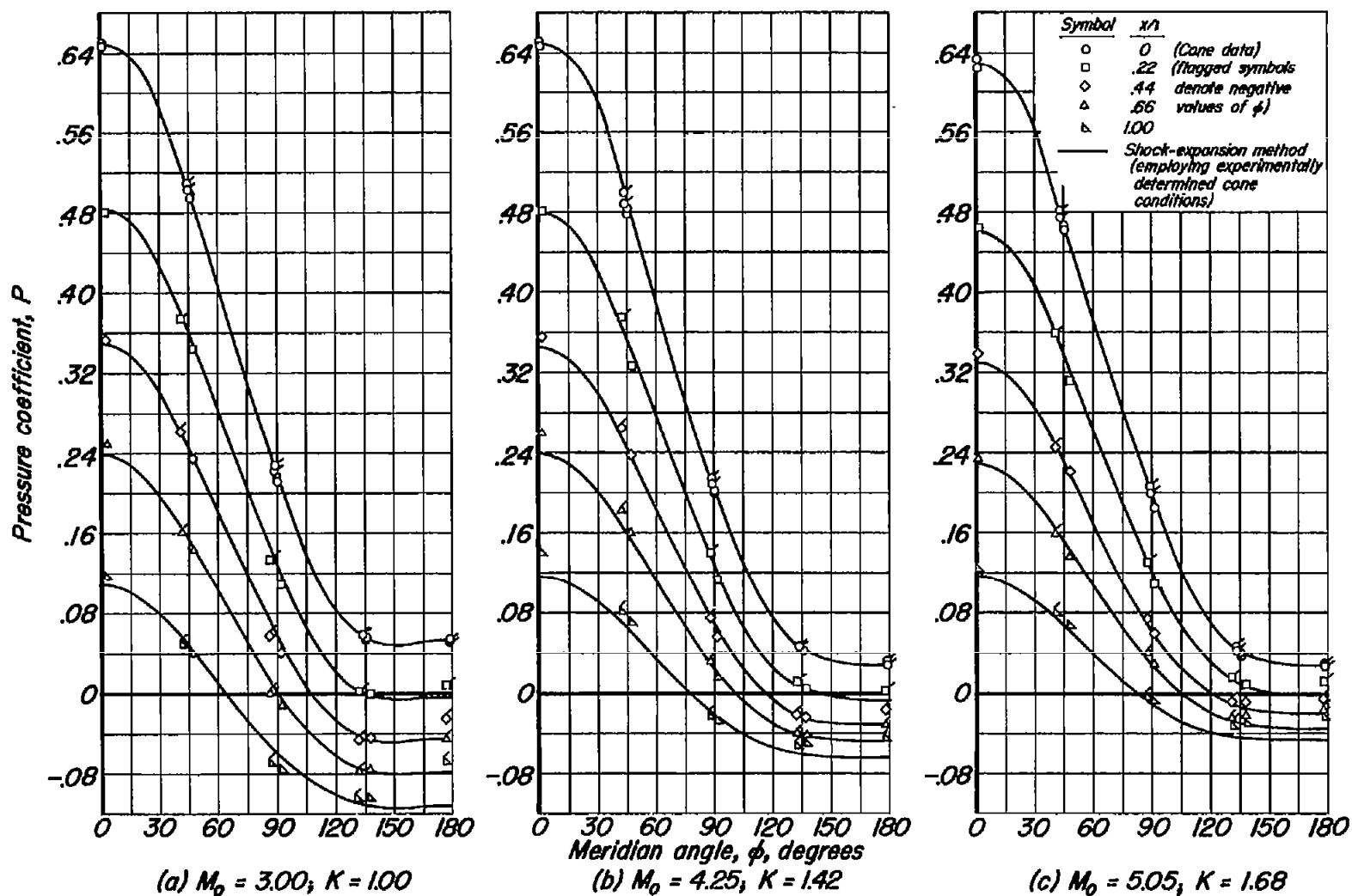


Figure 12.— Circumferential variation of pressure coefficient on a fineness ratio 5 ogive at  $\alpha = 15^\circ$



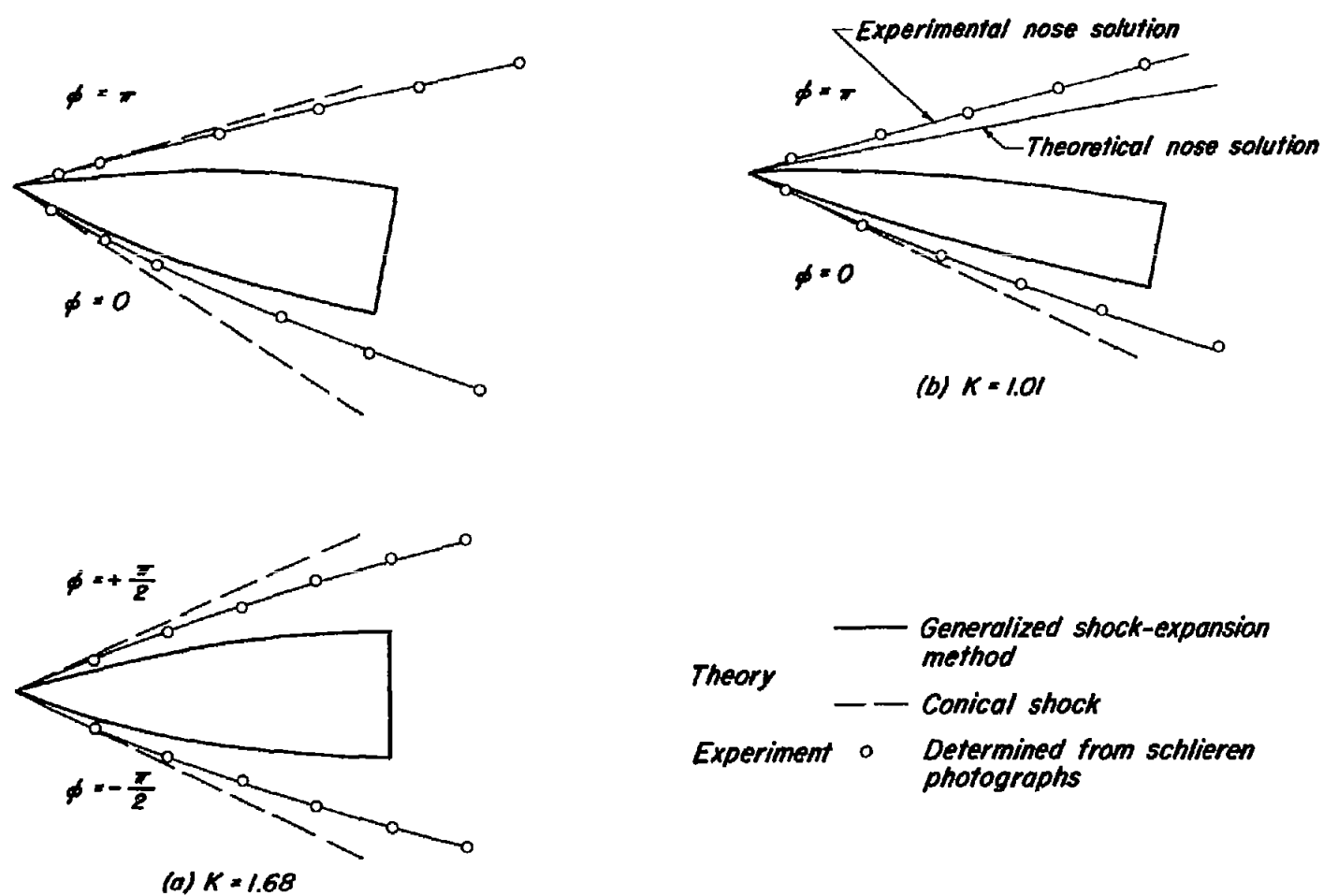


Figure 14.— Shock-wave shapes for ogives at two values of the similarity parameter,  $K$ ;  $M_0 = 5.05$ ,  $\alpha = 10^\circ$ .

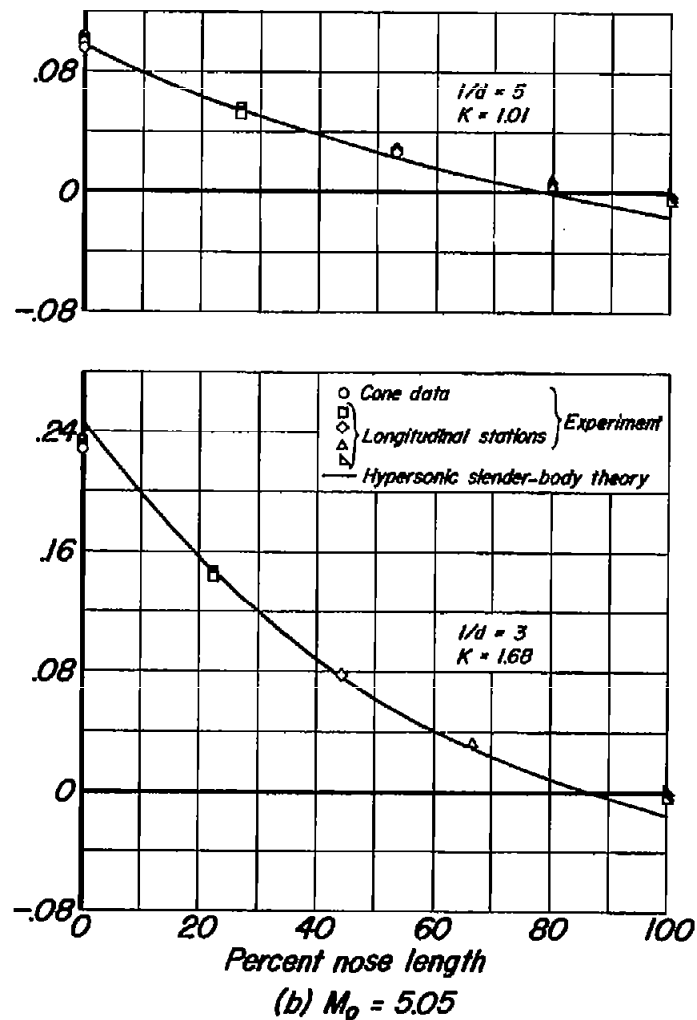
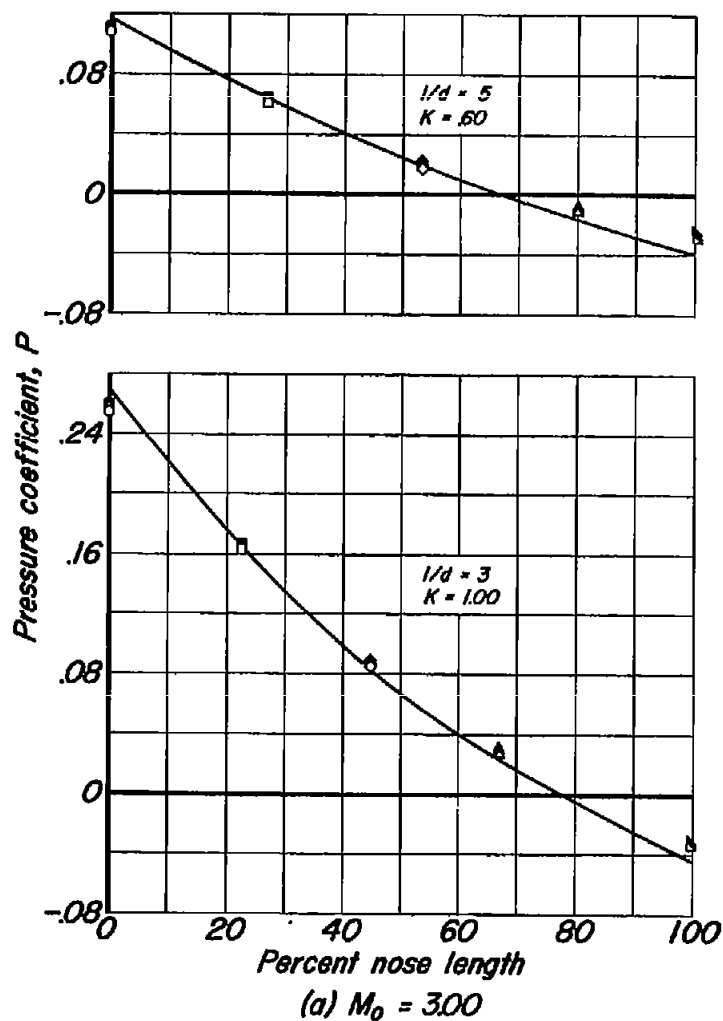


Figure 15.— Pressure distributions predicted by hypersonic slender-body theory for cgives at  $\alpha = 0^\circ$

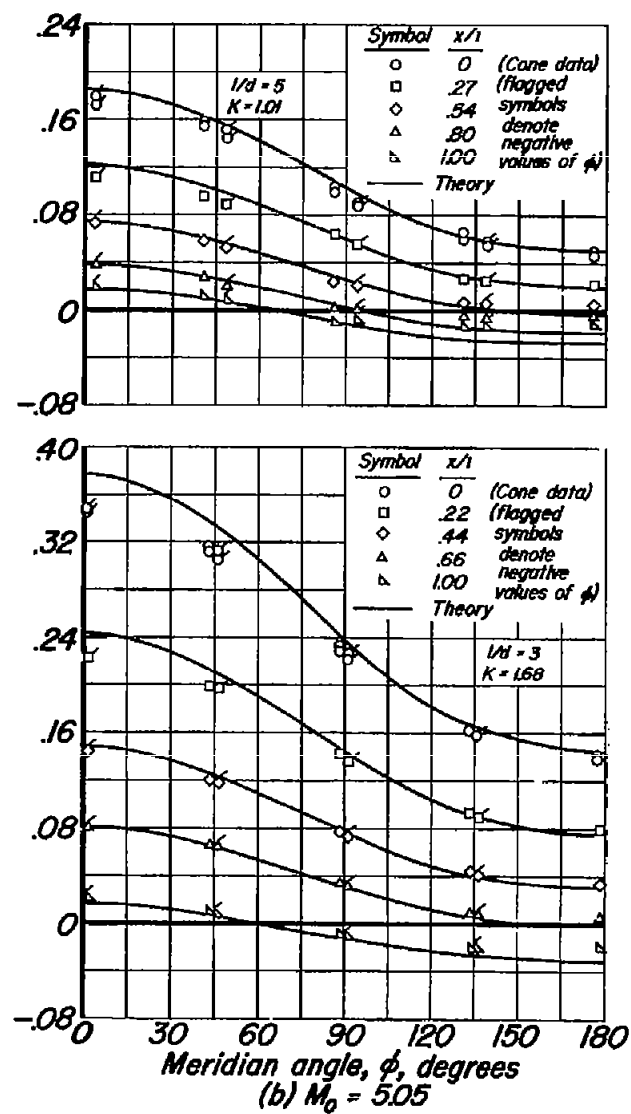
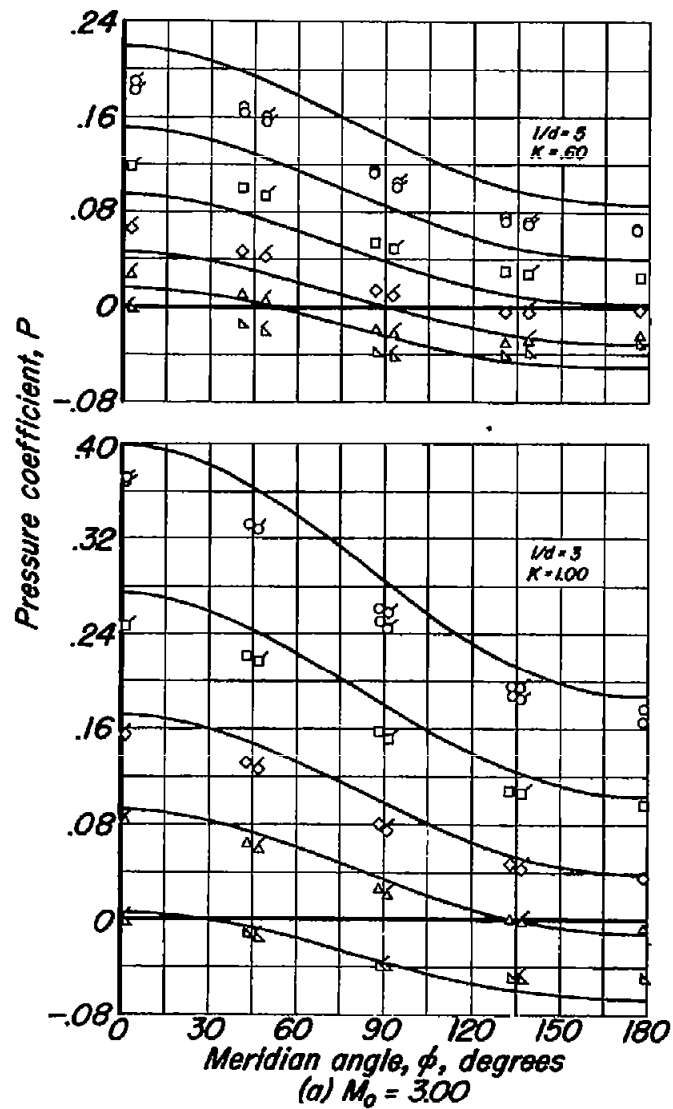


Figure 16.— Pressure distributions predicted by hypersonic slender-body theory for ogives at  $\alpha = 5^\circ$

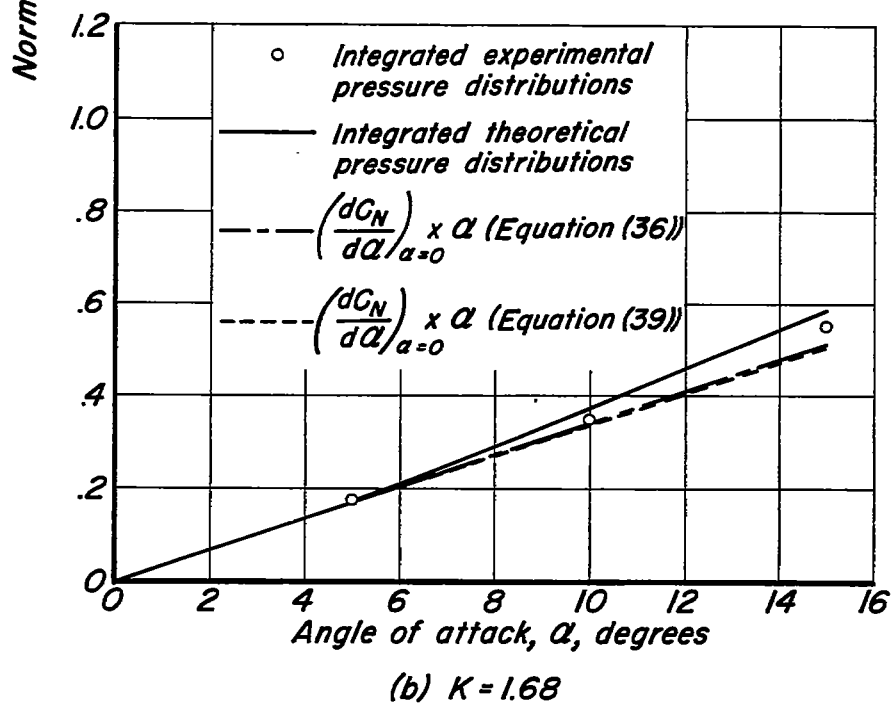
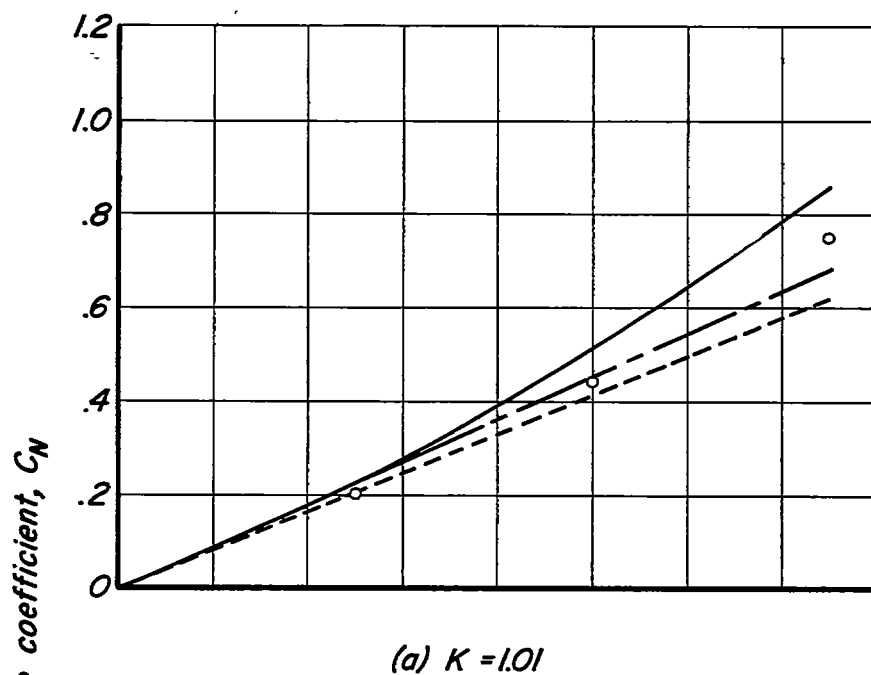


Figure 17.— Normal-force coefficients for ogives at  $M_0 = 5.05$ .